



Missouri University of Science and Technology
Scholars' Mine

AISI-Specifications for the Design of Cold-Formed Steel Structural Members

Wei-Wen Yu Center for Cold-Formed Steel Structures

01 Aug 2016

Characterization of CFS Framed Diaphragm Behavior

American Iron and Steel Institute

Follow this and additional works at: <https://scholarsmine.mst.edu/ccfss-aisi-spec>

 Part of the [Structural Engineering Commons](#)

Recommended Citation

American Iron and Steel Institute, "Characterization of CFS Framed Diaphragm Behavior" (2016). *AISI-Specifications for the Design of Cold-Formed Steel Structural Members*. 154.
<https://scholarsmine.mst.edu/ccfss-aisi-spec/154>

This Technical Report is brought to you for free and open access by Scholars' Mine. It has been accepted for inclusion in AISI-Specifications for the Design of Cold-Formed Steel Structural Members by an authorized administrator of Scholars' Mine. This work is protected by U. S. Copyright Law. Unauthorized use including reproduction for redistribution requires the permission of the copyright holder. For more information, please contact scholarsmine@mst.edu.

research report

**Characterization of
CFS Framed Diaphragm
Behaviour**

RESEARCH REPORT RP16-2

August 2016



American Iron and Steel Institute

DISCLAIMER

The material contained herein has been developed by researchers based on their research findings and is for general information only. The information in it should not be used without first securing competent advice with respect to its suitability for any given application. The publication of the information is not intended as a representation or warranty on the part of the American Iron and Steel Institute or of any other person named herein, that the information is suitable for any general or particular use or of freedom from infringement of any patent or patents. Anyone making use of the information assumes all liability arising from such use.



**DEPARTMENT OF CIVIL ENGINEERING & APPLIED
MECHANICS**

TECHNICAL REPORT

***CHARACTERIZATION OF CFS FRAMED DIAPHRAGM
BEHAVIOUR***

AISI PROJECT NUMBER CM - 432

Experimental Program Summer 2015

by:

Violetta Nikolaidou

Patrick Latreille

SUPERVISORS:

Prof. Colin A. Rogers

Prof. Dimitrios G. Lignos

This Report was prepared for the AISI Seismic Code Team

Abstract

Knowledge of the in-plane response to loading of cold-formed steel (CFS) framed diaphragm structures is essential for seismic and wind design. The information available specific to diaphragm design in the North American CFS design standards (AISI S240 & S400) is based on limited experimental work and the extrapolation of design methods developed for the wood industry. To address this shortcoming a test-based research project was performed in the Jamieson Structures Laboratory at McGill University focusing on the characterization of the behaviour under in-plane loading of CFS framed - wood sheathed diaphragms. This research was a complementary study to a research project involving the dynamic testing of CFS framed buildings, known as the CFS – NEES project. This Johns Hopkins University project involved full-scale two storey CFS framed buildings tested on a shake table under earthquake loading. Although the CFS – NEES project provided for the first time an insight into the seismic response of CFS structures, more information is required regarding the response of isolated diaphragm systems.

The research reported herein included diaphragm test specimens that were based on the floor and roof configurations used in the CFS - NEES Building; which were comprised of oriented strand board (OSB) sheathing screw connected to CFS C-Channel joists. The cantilever diaphragm test approach was followed and the specimen dimensions were chosen considering the AISI S907 Standard requirements. Four diaphragm configurations were selected, each of which was tested under in-plane monotonic and reversed cyclic loading, resulting in a total of eight test specimens. A self-reacting frame was initially designed and constructed as a test-setup in order to accommodate the 12'x 24' (3.66 m x 7.31 m) diaphragm specimens. It was demonstrated that screw size constitutes a decisive factor in the resulting diaphragm response. In addition, the fully blocked diaphragm configurations, i.e. where the edges of all sheathing panels are supported by an underlying CFS frame, exhibited a considerable increase in shear strength. The bare steel frame contribution to shear strength and stiffness was negligible. An effort to predict the shear strength and deflection of the diaphragm specimens was made using the information available in the AISI S400 Standard. However, the limited information provided in the aforementioned Standard prevented a meaningful comparison to be realized between the predicted design values and the measurements from the tests.

Acknowledgements

The authors would like to thank the American Iron and Steel Institute (AISI) for financially supporting this research project. Additional support was obtained from the Canadian Sheet Steel Building Institute (CSSBI) and the Natural Sciences and Engineering Research Council of Canada (NSERC). A special thank you is also extended to Bailey Metal Products Ltd., Simpson Strong-Tie Co. Inc., Ontario Tools and Fasteners Ltd, ArcelorMittal and Construction Proco Inc. for the materials and tools that have been provided.

The research was sponsored by the American Iron and Steel Institute (Project number CM-432) and this report was prepared for the AISI Seismic Code Team.

Table of Contents

Abstract.....	i
Acknowledgements	ii
Table of Contents	iii
List of Tables	v
List of Figures.....	vi
1 – Introduction.....	1
2 – Background	1
3 – Objectives.....	4
4 – Scope.....	4
5 – Description of Test-Setup and Specimens.....	5
5.1 Test-Setup	5
5.2 Diaphragm Configurations	8
5.2.1 Part 1	9
5.2.2 Part 2	13
6 – Instrumentation	14
7 – Material Properties	16
7.1 Coupon Tensile Tests of Steel	16
7.2 Moisture Content Measurements of OSB Panels	18
8 – Diaphragm Experimental Results	19
8.1 Part 1 Diaphragm Tests.....	19

8.1.1 Loading Protocol	19
8.1.2 Test Results	21
8.2 Part 2 Diaphragm Tests.....	25
8.3 Comparison of Part 1 and Part 2 Diaphragm Response to Loading	29
9 – Design Predictions.....	32
9.1 Deflection.....	32
9.2 Shear Resistance	41
10 – Conclusions.....	43
11 – References	45

List of Tables

Table 1	Diaphragm configurations	12
Table 2	Specimen nomenclature.....	14
Table 3	Tensile coupon test results.....	18
Table 4	OSB moisture content measurement	19
Table 5	Reversed cyclic loading protocol of roof configuration	20
Table 6	Summary of shear resistance results.....	32
Table 7	Comparison of measured displacement at ultimate load versus calculated deflection using Equation 1.2 with δ_v maximum	34
Table 8	Comparison of displacement based on initial linear elastic stiffness versus calculated deflection using Equation 1.2 with δ_v elastic	38
Table 9	Comparison of displacement based on initial linear elastic stiffness versus calculated deflection using Equation 1.3.....	41
Table 10	Comparison of measured and nominal shear resistance	41

List of Figures

Figure 1	CFS - NEES building (Peterman 2014).....	3
Figure 2	3D representation of diaphragm test-setup	6
Figure 3	Test frame construction and connection details	7
Figure 4	Diaphragm connections	9
Figure 5	3D illustration of diaphragm configuration	10
Figure 6	Diaphragm specimens attached to test-setup.....	11
Figure 7	Wall detail (Madsen et al. 2011)	11
Figure 8	# 8 and # 10 screws.....	12
Figure 9	OSB panel grade stamps.....	12
Figure 10	Diaphragm modifications for Part 2 of experimental program	13
Figure 11	Instrumentation	15
Figure 12	Tensile coupon testing process	17
Figure 13	Typical engineering stress – strain curve of steel.....	17
Figure 14	Reversed cyclic loading protocol of roof configuration.....	20
Figure 15	Shear force vs. rotation response for the bare steel frame of diaphragm roof and floor configurations No. 1 & 2	21
Figure 16	Shear force vs. rotation response for Part 1 diaphragm roof specimens No. 3 & 4.....	22
Figure 17	Deformation for Part 1 diaphragm roof specimens No. 3 & 4	23
Figure 18	Shear force vs. rotation response for Part 1 diaphragm floor specimens No. 5 & 6	24

Figure 19	Deformation for Part 1 diaphragm roof specimens No. 3 & 4	25
Figure 20	Shear force vs. rotation response for Part 2 diaphragm roof specimens No. 7 & 8.....	26
Figure 21	Deformation for Part 2 diaphragm roof specimens No. 7 & 8	27
Figure 22	Shear force vs. rotation response for Part 2 diaphragm roof specimens No. 9 & 10.....	28
Figure 23	Deformation for Part 2 diaphragm roof specimens No. 9 & 10	28
Figure 24	Shear force vs. rotation response for fully blocked versus unblocked roof diaphragm	29
Figure 25	Shear force vs. rotation response for #12 versus #10 sheathing screws floor diaphragm	31
Figure 26	Table A used to find G_{vt} in order to approximate shear modulus, G (TECO, 2008)	35
Figure 27	Elastic deflection as obtained from elastic shear force vs. rotation curve.....	38
Figure 28	Table D2-1 in AISI S213 (2007) or Table F2.4-1 in AISI S400 (2015)	42

1- Introduction

In recent years, there has been an increase in the construction of cold-formed steel (CFS) framed multi-storey residential and commercial buildings. Current code provisions addressing the seismic design of CFS framed structures (AISI S400, AISI S100, ASCE 7, CSA S136 and NBCC 2010) are based on the response of the bare steel shear walls, as the main lateral force resisting elements. Response modification coefficients R in the U.S., as well as the equivalent R_d and R_o seismic force modification factors in Canada, accounting for the ductility and over-strength, do not explicitly take into account the floor and roof diaphragms' contribution to the lateral resistance and dynamic response of the structure. At present in the AISI S400 Standard (2015), there is no Canadian design procedure available for diaphragms in CFS framed structures; and as for the US design provisions for diaphragms, there has been limited research behind their development. Moreover, the influence of the diaphragm's relative stiffness on the overall seismic response and transfer of forces in the structure has yet to be characterized and considered in design, i.e. of the diaphragm connection to the shear walls. Comparing with the design guidelines provided for the seismic design of structures by the hot-rolled steel and concrete codes, the design deficiencies of the CFS building design provisions become evident. As such, there exists a need for this shortcoming to be addressed in order to ensure the construction of better, safer and more economic CFS structures.

This technical report presents in detail the research project realized in the Jamieson Structures Laboratory at McGill University during the summer of 2015 aimed at the characterization of CFS framed - wood sheathed diaphragm behaviour under in-plane loading. It constitutes the first step of an ongoing research program that includes both experimental and numerical work with the purpose of improving design provisions for CFS framed diaphragms for use in Canada and the United States.

2- Background

One of the early researchers focusing on the diaphragm design for CFS structures was Lum (LGSEA 1998). Lum provided allowable design strength values for plywood sheathed CFS framed diaphragms using the National Design Specification (NDS 1991) formulas for the

fastener resistance and the methodology by Tissell and Elliot (2004) for wood framing to calculate the diaphragm's ultimate shear strength. These design values were originally included in Table C2-1 of the AISI S213 Standard (2007) and now are available in Table F2.4-1 of the new AISI S400 Standard (2015). CFS framed - wood sheathed diaphragm configurations were also tested by the National Association of Home Builders Research Center (NAHBRC 1999) and the individual fastener response was examined. Included in the test program were four 3.6x7.2m (12'x24') unblocked simple span diaphragm specimens with 18.3mm (23/32in) wood sheathing connected with #8 screws (152.4/304.8mm (6"/12") in spacing pattern) to CFS C-channel perforated joists (joist sections varied per two specimens). The loading protocol consisted of two monotonic loading cycles (loading, unloading and loading again towards one direction) before pushing the diaphragm to failure. The maximum load reached during the tests was 18.9 kN/m. Results showed that by multiplying the individual screw connection shear capacity with the number of fasteners along one end of the diaphragm provides a good estimate of the diaphragm's shear capacity. Valuable information on diaphragm seismic response is also provided by extensive experimental work on wood framed shear walls and diaphragms, e.g. Dolan and Madsen (1992), Tissell and Elliot (2004), and Brignola et al. (2012).

Moreover, during the last three years an ongoing major research program was being realised at Johns Hopkins University, entitled "Enabling Performance-Based Seismic Design of Multi-Story Cold-Formed Steel Structures" (Peterman 2014), involving full size two-storey CFS wood sheathed shear wall buildings tested under earthquake loading using the Network for Earthquake Engineering Simulation (NEES) equipment site (shake table) at the State University of New York (SUNY) at Buffalo in the USA (Figure 1). A full description of the criteria used for the design of the CFS shear walls and diaphragms of the test structure can be found in Madsen et al. (2011). The main parts of this research program were: (1) the investigation of the response of isolated CFS framed - wood sheathed shear walls and of the stud-fastener-sheathing connection under cyclic loading through experimental work, and (2) the characterization of the response and design of the overall CFS framed structure under seismic loading through the means of shake table tests and finite element modeling (Schafer et al. 2014). Isolated wood sheathed CFS framed shear walls were tested using monotonic loading and the CUREE (Krawinkler et al. 2000) loading protocol (Liu et al. 2012). In Leng et al. (2013), based on the aforementioned shear wall

testing (Liu et al. 2012), dynamic and non-linear response history analyses were conducted in order to simulate the response of the two-storey CFS framed building tested at Buffalo using OpenSees (McKenna 1997). The diaphragm was assumed to be rigid in the simulation because test information was not available with which to assign a more realistic in-plane stiffness.



Figure 1: CFS - NEES building (Peterman 2014)

The National Building Code of Canada (NRCC 2010) refers to the CSA S136 Standard (2007) for the design of cold-formed steel structures. In turn, CSA S136 refers to the AISI S213 Standard (2007) for the design guidelines of CFS framed structures under lateral loading. In the US the AISI S213 Standard is specified for the lateral design of CFS framed structures through the ASCE 7 and the building code under which the building is designed. AISI S213, now replaced by AISI S400, provides US design shear strength values for specific CFS framed diaphragm configurations (LGSEA 1998), while for any other diaphragm assembly it indicates that principles of mechanics must be employed for the shear strength calculation. The diaphragm deflection equation D2.1 included in the AISI S213 Standard is based on that derived for simply supported wood-framed diaphragms, with slight modifications making it applicable for steel-framed structures (Serrette and Chau 2003).

At present, the AISI S400, NBCC 2010 and CSA S136 standards do not address the seismic design of wood sheathed / CFS framed diaphragms for use in Canada. Moreover, the existing R_d , R_o values used for the seismic design of CFS structures do not include the diaphragm's contribution. Similarly, the US response modification coefficients for CFS structures found in ASCE 7 do not explicitly account for the influence of the diaphragm. From the above-mentioned

literature, it is highlighted that, although a considerable number of studies exist for CFS framed shear walls, limited information is provided regarding the entire CFS framed building response including diaphragm flexibility and diaphragm-to-shear wall connection flexibility. Although, the AISI S213 Standard was replaced in 2015 by AISI S400 (2015) for seismic related design provisions and AISI S240 (2015) for wind related design provisions, no modifications with respect to diaphragm design were incorporated in these two new standards.

3- Objectives

The main objective of the research described in this report is to characterize the behaviour of CFS framed roof and floor diaphragms under monotonic and reversed cyclic in-plane loading. A secondary objective is to compare the measured test results with predictions of resistance and displacement determined from the existing provisions in AISI S400.

4- Scope

Given the complexity of diaphragm system behaviour under loading, due to the use of various configurations, different materials, non-linear fastener response, etc., in order for strength and stiffness properties to be established large-scale monotonic and reversed cyclic testing is typically required. To this end, a test-setup (self-reacting frame) was designed, fabricated and installed in the structures laboratory in order to conduct diaphragm tests. The design load for the frame was based on the maximum capacities of previous diaphragm and shear wall tests found in the aforementioned literature and the equipment available in the McGill structures laboratory (i.e. the actuator used).

Two diaphragm specimen configurations based on those used in the CFS - NEES building (Figure 1), as described by Madsen et al. (2011) and Peterman (2014), were selected for the experimental program described in this report. Two additional configurations were chosen to improve upon the response to loading offered by the original diaphragm construction. All diaphragm specimens were composed of oriented strand board (OSB) sheathing screw fastened to CFS C-Channel joists. The cantilever test approach was followed and the specimen dimensions 3.66 x 6.1m (12' x 20') were chosen in consideration of the AISI S907 Standard (2013) requirements. Each diaphragm configuration was subjected to a monotonic and a CUREE

reversed cyclic (Krawinkler et al. 2000) displacement controlled loading protocol, leading to the testing of a total of eight diaphragm specimens in the scope of this research project. In addition to a reporting of the testing and test results, this document contains a comparison between the measured shear strength values and the corresponding design values included in AISI S213 2007 / S400 2015, as well as a comparison with deflection estimates using equation C2.1 of the S213 Standard (Eq. E1.4.1.4-1 in AISI S400).

5- Description of Test-Setup and Specimens

This section contains a description of the diaphragm configurations that were tested and the loading protocols that were used; and further includes a brief description of the test-setup designed to accommodate the tests.

5.1 Test-Setup

The idea behind the construction of this prototype frame was to provide a test-setup that can accommodate both the current testing program included in this report and future experimental work on diaphragms. SAP2000 commercial software (CSI 2009) was relied upon in order to analyse and design the test frame. A self-reacting braced frame configuration was chosen comprised of three pin connected short beams, two long continuous beams and four pin connected braces. A conservative approach was followed to determine the design load, which was based on the capacities exhibited from CFS and wood shear walls and diaphragms of past experimental programs described in the literature review, as well as on the maximum capacities observed from sheathed CFS framed shear wall testing performed at McGill University (Branston 2004, Chen 2004, Boudreault 2005, Rokas 2005 and Blais 2006). The maximum load applied to the diaphragm specimens was predicted to be not greater than 200KN. The actuator chosen for this application has a tensile capacity of 450KN and compressive capacity of 650KN. It was decided to design the test frame based on the actuator's tensile capacity. A safety factor of 1.2 was implemented leading to a maximum load of 540KN considered for design, which is almost three times higher than the maximum diaphragm testing load observed in the literature. Based on the diaphragm specimens' plan dimensions, the overall frame dimensions were chosen to be 4.5x6.5m (15'x 22') (Figure 3). A uniform load of $540/6.1=88.5$ kN/m was applied in the

SAP2000 model on the side where the diaphragm was bolted while a roller support was placed in the location of the actuator restraining the x-direction degree of freedom. This support simulated the reaction force applied on the frame from the actuator. A maximum shear capacity of 50KN was assumed for the anchor rods to be used. However, most of the in-plane forces should be contained within the frame and not transferred to the strong floor; thus, four roller supports were implemented in the SAP2000 model restricting the y-direction while allowing the free movement of the frame in the x-direction as would be expected based on the applied loading. The frame sections were chosen so that the frame remains elastic throughout the testing process and has adequate stiffness to exhibit the minimum possible deformation. It was expected that the design was mainly based on maximum deformations allowed and not on member capacities; thus a limit of $L/1125$ (4mm or 0.157") was used, where $L=4.5\text{m}$ (15'). Figure 2 displays the test-setup.

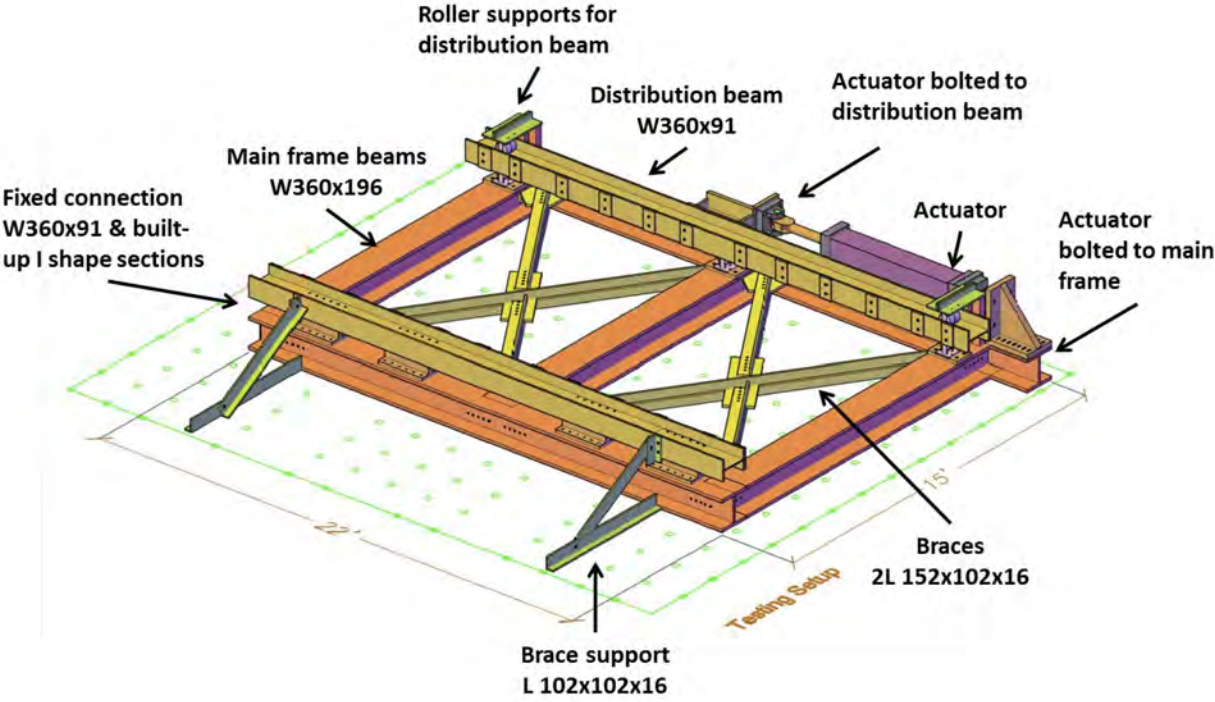


Figure 2: 3D representation of diaphragm test-setup

The frame sections were: W360x196 (W14 x 132) sections for the beams and 152x102x16 (6 x 4 x 5/8) angle sections with 25.4mm (1") spacing for the braces. A W360x91 (W14 X 61) load distribution beam was bolted to the actuator and the rim-joint of the diaphragm specimen in order to distribute the concentrated force from the actuator to the diaphragm. Rollers at the top and

bottom support the distribution beam in three locations (edges and middle). This roller system allowed in-plane rotation of the diaphragm (movement perpendicular to actuator) during the test. The actuator was in turn bolted to the main frame; however, each end of the actuator comprises a swivel mount which also allowed for in-plane perpendicular movement of the load distribution beam. An extra roller support was added under the actuator in the middle to account for the possible eccentric vertical loading on the distribution beam caused by the actuator's self-weight. A fixed connection was created on the other side of the frame by bolting four built-up I shape sections to the main frame and a W360x91 (W14 x 61) reaction beam, which was bolted in turn to the rim joist of the diaphragm specimen. Braces were also installed and connected to the strong floor to support the fixed connection against potential rotation during the test. It should be noted that the designed testing setup involved the diaphragm being connected in only two locations with hot rolled steel beams (fixed connection and distribution beam) without any extra steel elements supporting the CFS framing, as is the norm in classic metal panel cantilever tests. Figures 3 a, b, c, d, e & f depict the various connections and parts of the test-setup. It is worth mentioning that, during testing, the test-setup fulfilled its purpose as a self-reacting frame. Based on the instrumentation set in place as explained in Section 6, the in-plane forces were taken by the frame and not the anchor rods; further, there was no displacement observed by the test frame with respect to the strong floor throughout the testing process.



(a) Test frame

Figure 3: Test frame construction and connection details



(b) Test frame with specimen framing



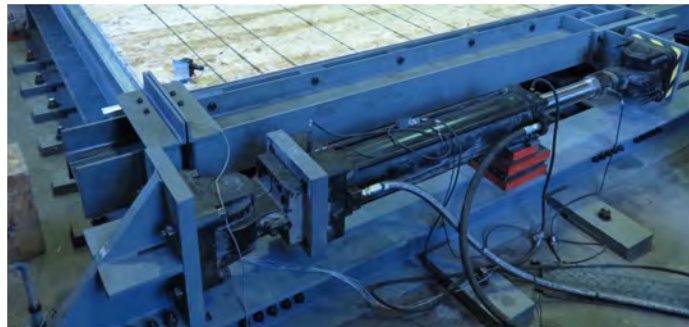
(c) Roller supports of distribution beam



(d) Brace to main beams



(e) Fixed connection



(f) Actuator to distribution beam and main frame

Figure 3 (Continued): Test frame construction and connection details

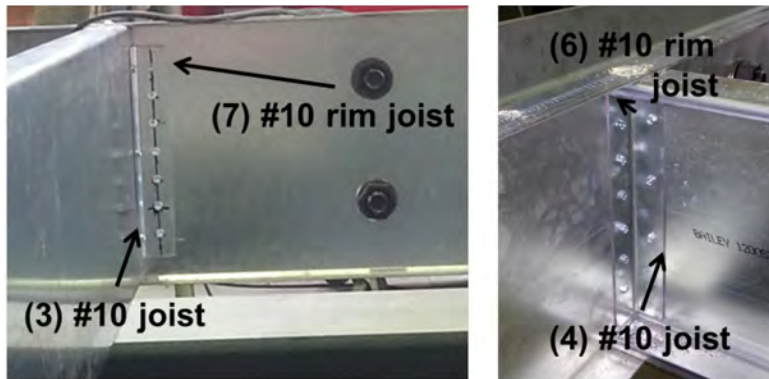
5.2 Diaphragm Configurations

The experimental program consisted of two parts. The first part involved two main diaphragm configurations chosen based on the configurations used in the CFS - NEES building (Figure 1) for the floor and roof assembly, while the second part involved the same configurations with modifications. In total, eight tests were conducted, four with monotonic and four with reversed

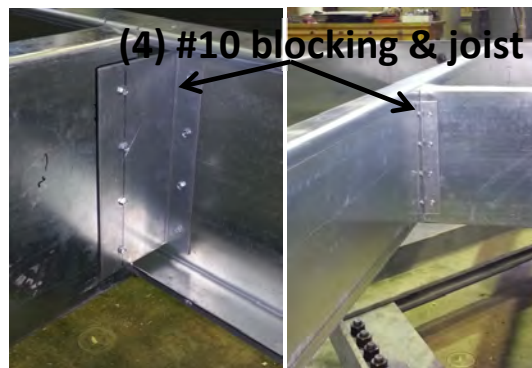
cyclic loading. An additional two monotonic tests for the bare steel framing of the two main diaphragm configurations were also included.

5.2.1 Part 1

Table 1 summarizes the two basic diaphragm configurations. Joist, rim joist and blocking sections as well as joist to rim joist connections and blocking to joist connections were based on the roof diaphragm and floor diaphragm used in the CFS - NEES building (Figure 1, Madsen et al. 2011). Straps were used connecting the blocking sections together in order to provide lateral support to all the joists. Figures 4a, b and c illustrate the connections for the floor and roof configurations, depicting the number of screws used in parenthesis followed by their size (i.e. (7) # 10 refers to 7 screws used of #10 size).



(a) Roof rim joist to joist connection (b) Floor rim joist to joist connection



(c) Blocking connection to joist for both configurations

Figure 4: Diaphragm connections

Figure 5 includes a 3D illustration of the specimens, while Figure 6 demonstrates the specimens attached to the test-setup. It should be noted that in order to include the stiffening effect of a wall attached to the diaphragm an extra joist was added to each end of the specimen (double joist chords). Moreover, the wood panels in the CFS - NEES building extended 6in (152 mm) inside the wall as shown in Figure 7 (Madsen et al. 2011); thus, for reasons of consistency the sheathing panels in this testing program also extended 6in (152 mm) past the rim joist (carrier track) along the fixed connection location of the diaphragm. Thus the out-to-out dimension of the CFS frame was 11'6" (3505 mm). The screws used for each case are indicated in Table 1 and are also shown in Figure 8. The sheathing screws spacing was 152mm (6in) o/c at the panel edges when supported by joists or blocking and 305mm (12in) o/c in the field. Figure 9 displays the grade stamps of the OSB panels.

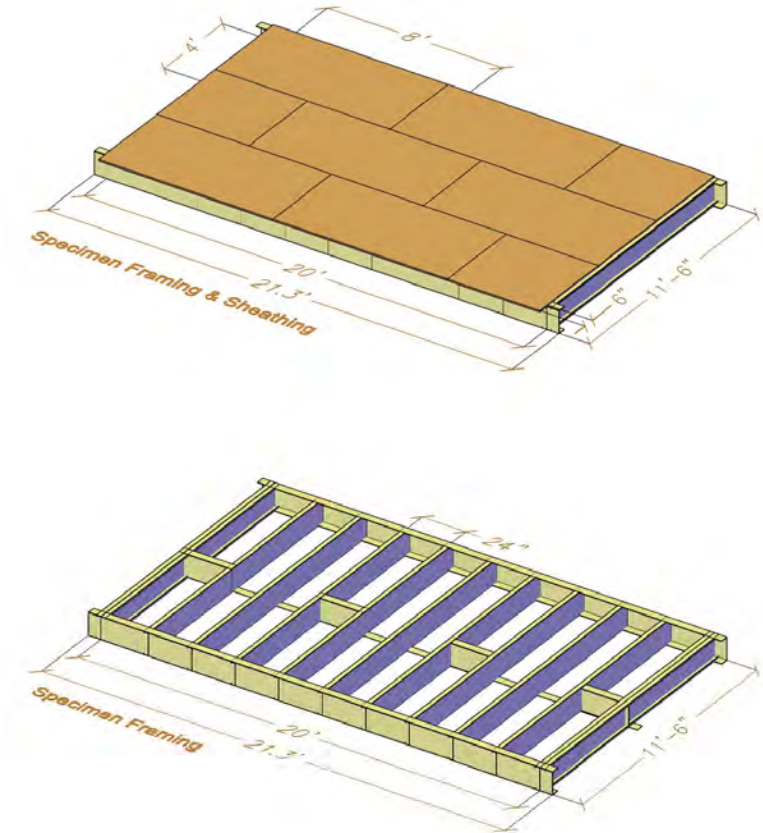
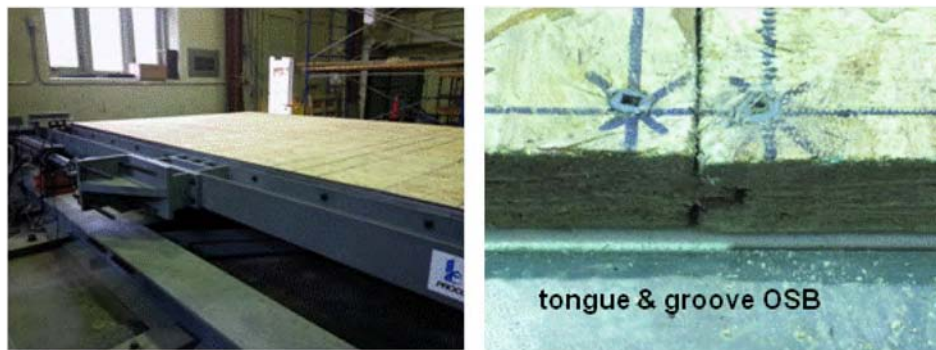


Figure 5: 3D illustration of diaphragm configuration



(a) Roof configuration



(b) Floor configuration

Figure 6: Diaphragm specimens attached to test-setup

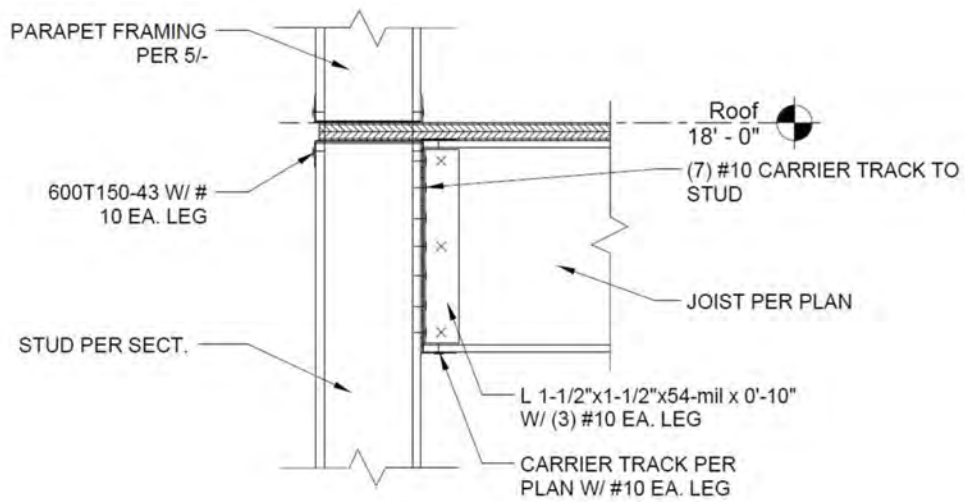


Figure 7: Wall detail (Madsen et al. 2011)

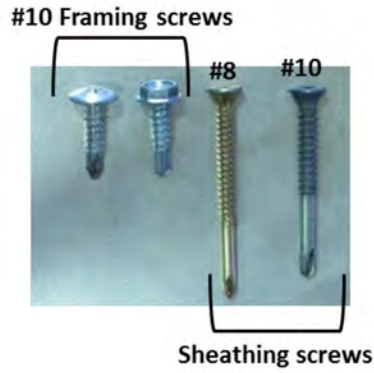


Figure 8: #8 and #10 screws



Figure 9: OSB panel grade stamps

Table 1: Diaphragm configurations

Configuration Roof (Gr. 50)	Section	Length
Joists	1200S200-54	11' 6"
Rim Joists	1200T200-68	21' 3"
Web Stiffeners	L 1-1/2"x1-1/2"x54	10"
Blocking	1200S162-54	22"
Blocking Connectors	L 1-1/2"x 4" x54	10"
Straps	1-1/2"x54	20' 8"
#8 sheathing self-drilling (6"/12" spacing)	-	1-1/4"
#10 steel-to-steel flat head self-drilling	-	3/4"
#10 steel-to-steel Hex Head Cap self-drilling	-	1"
OSB panels (24/16 rated)	8' x 4' x 7/16"	-

Table 1 (Continued): Diaphragm configurations

Configuration Floor (Gr. 50)	Section	Length
Joists	1200S250-97	11' 6"
Rim Joists	1200T200-97	21' 3"
Web Stiffeners	L 1-1/2"x1-1/2"x54	11"
Blocking	1200S200-54	21-1/2"
Blocking Connectors	L 1-1/2"x 4" x54	10"
Straps	1-1/2"x54	20' 8"
#10 sheathing self-drilling (6"/12" spacing)	-	1-1/2"
#10 steel-to-steel flat head self-drilling	-	3/4"
#10 steel-to-steel Hex Head Cap self-drilling	-	3/4"
OSB panels (48/24 rated)	8' x 4' x 23/32"	-

5.2.2 Part 2

In the second part of the laboratory test program a fully blocked roof configuration was used, i.e. the perimeter of each panel was fastened at 152 mm (6in) o/c to an underlying CFS frame, to address the observed failures in the first tests (Section 8.1). While for the floor configuration #12 sheathing screws were used instead of #10 screws to account for the fastener failures observed in the first tests (Section 8.1). Figure 10 contains photographs of these changes for the two diaphragm configurations.



Figure 10: Diaphragm modifications for Part 2 of experimental program

Through these changes the effect of blocking and size of screws on the diaphragm capacity and ductility was investigated. More details are provided in Section 6.2 of this report. Table 2 provides the nomenclature of the specimens used throughout this report.

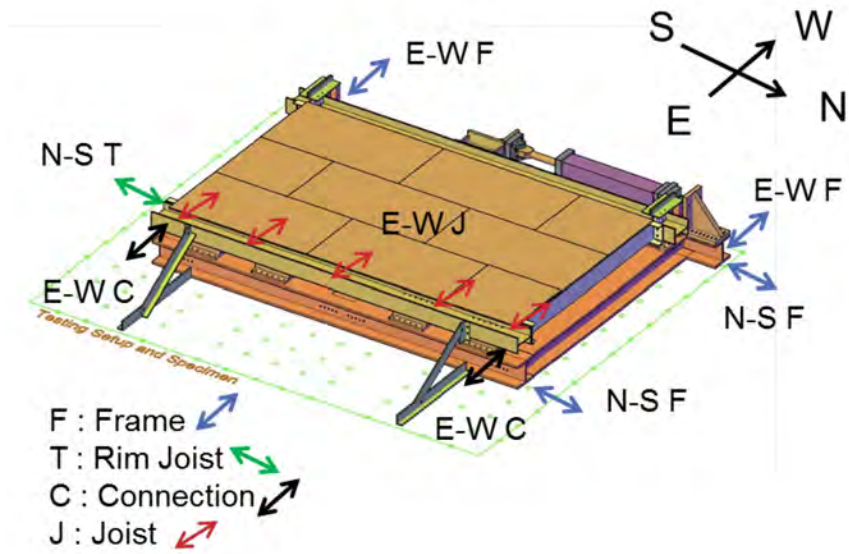
Table 2: Specimen nomenclature

Specimen	Description
No.1	Roof Bare Steel Frame Monotonic
No.2	Floor Bare Steel Frame Monotonic
No.3	Roof Unblocked Monotonic
No.4	Roof Unblocked Cyclic
No.5	Floor #10 Screws Monotonic
No.6	Floor #10 Screws Cyclic
No.7	Roof Blocked Monotonic
No.8	Roof Blocked Cyclic
No.9	Floor #12 Screws Monotonic
No.10	Floor #12 Screws Cyclic

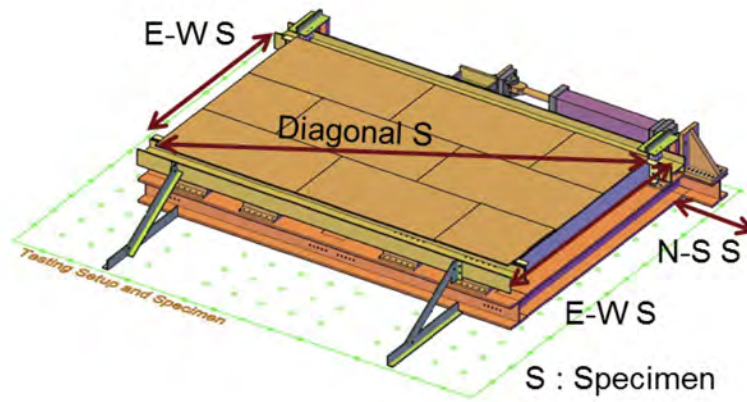
6- Instrumentation

The instrumentation included four string potentiometers to capture the lateral displacement of the specimen and the overall shear deformation (254mm (10in) & 508mm (20in) stroke), 12 linear variable differential transformers (LVDTs, ± 15 mm (3/5in) stroke) measuring in-plane displacement locally and strain gauges attached at the end joists in an effort to measure the axial force of the chords. In addition, the actuator was equipped with an internal LVDT and a load cell. Figure 11a, b and c indicate the locations of the instruments.

The purpose of the instrumentation installed on the diaphragm specimens and on the test-setup was to capture the shear deformation of the diaphragm, any slippage detected of the rim joist connection to the reaction beam and the joist deformation relative to the test-setup, as well as any movement of the test-setup relative to the strong floor. The measurement instruments were connected to Vishay Model 5100B scanners that were used to record data using the Vishay System 5000 StrainSmart software.



(a) LVDTs



(b) String potentiometers



(c) Strain gauges

Figure 11: Instrumentation

7- Material Properties

Coupon tensile testing of the cold-formed steel frame was realized and moisture content measurements of the OSB panels were taken. The following subsections provide details on these ancillary tests.

7.1 Coupon Tensile Tests of Steel

Tensile coupon specimens were extracted from the CFS joist and rim joist sections as per the ASTM A370 Standard (2007) with 50mm gauge length. Three coupons were provided for each steel thickness (roof rim joist, roof joist, floor rim joist, floor joist). For the second part of testing, extra coupon specimens were tested, cut from the floor and roof joists, since these members came from different coils. After testing, half of the specimens were immersed in a solution of 15% hydrochloric acid and 85% water in order to remove the zinc coating and to measure the base metal thickness of the coupons. Figure 12 illustrates the 150 kN MTS machine used to test the coupons. In the elastic range the load rate was 0.002mm/s, which changed to 0.01mm/s once the curve reached the plateau region and then to 0.1mm/s once strain hardening was initiated. An extensometer with a gauge length of 50 mm was also attached to the middle of the specimen in order to measure the elongation. In addition, a visual method was also implemented where the coupons were punch-marked at 50.8 mm (2in) gauge distance in the middle of the specimen before the test and then the distance between these two points was measured again after the test had finished. Two strain gauges (one centered on each side) were also placed on one coupon of each set of three in order for the Young's modulus values to be obtained accurately. The nominal yield stress of steel was 345MPa (50ksi). A typical engineering stress-strain curve is shown in Figure 13 for JF1 (specimen from the joist of the floor configuration) along with the strain gauge data and the Young's modulus value. The specimens showed sharp yielding behaviour. Table 3 summarises the results from the tensile coupon tests.



Figure 12: Tensile coupon testing process

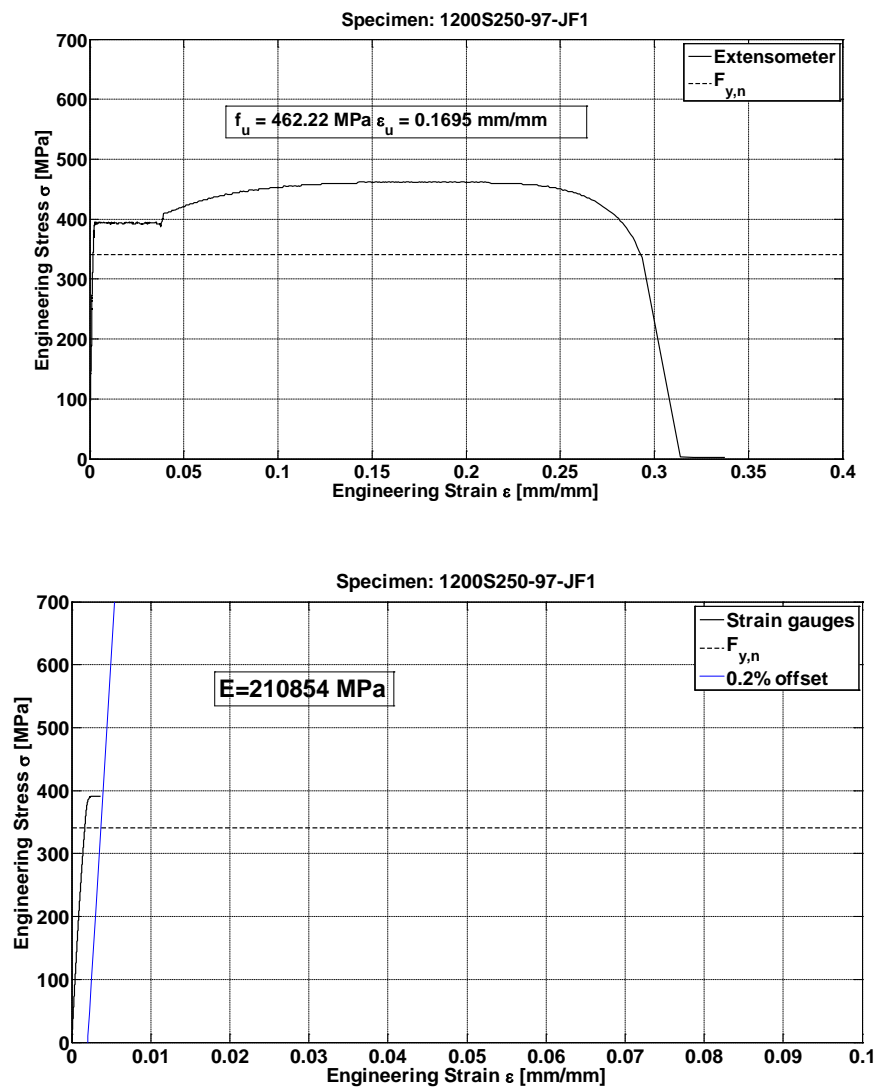


Figure 13: Typical engineering stress - strain curve of steel

Table 3: Tensile coupon test results

Specimens	E (MPa)	F _y (MPa)	ε _y (mm/mm)	F _u (MPa)	ε _u (mm/mm)	F _u /F _y	Elongation (%)	No.
Rim Joist Roof	188595	387	0.0040	466	0.1717	1.20	27.5	3
Rim Joist Floor	224149	398	0.0028	474	0.1822	1.19	31.8	3
Joist Roof	189049	391	0.0037	471	0.1959	1.20	28.7	3
Joist Floor	210854	394	0.0036	462	0.1695	1.17	29.3	1
Joist Roof 2	200568	385	0.0015	466	0.0673	1.21	14.8	3
Joist Floor 2	202097	410	0.0018	477	0.0858	1.16	14.6	3

The yield stress was calculated based on the autographic method, where two strain offset lines are used, at 0.4% and 0.8%. The yield stress is taken as the average of the two points of these lines intersecting the yield plateau of the coupon capacity curve. This method was deemed more appropriate for sharply yielding specimens, although the 0.2% offset for our case provided similar results.

7.2 Moisture Content Measurements of OSB Panels

Three round specimens per panel (76.2mm (3in) diameter) were extracted from a number of wood panels that had been used during testing for the roof and floor configuration. The specimens' weight (green mass) was measured immediately after testing and then the secondary oven-drying method of ASTM D4442 Standard (2007) was used (Method B) in order for their moisture content to be measured. According to this method, the specimens were placed for 24 hours in an oven under a constant temperature of 103°C in order for the oven dry mass to be obtained. Subsequently the moisture content (MC) was calculated (Equation 1.1, Table 4):

$$MC = \frac{\text{Initial weight} - \text{Oven-dry weight}}{\text{Oven-dry weight}} \times 100\% \quad (1.1)$$

It is shown that the moisture content for all the specimens is well below 15% ensuring that the wood properties were not influenced by wet conditions.

Table 4: OSB moisture content measurement

Wood Blocks		Green mass (g)	Oven dry Mass (g)	MC (%)	Average MC (%)
CR	1	59.22	57.25	3.4	3.6
	2	43.47	41.79	4.0	
	3	56.78	55.00	3.2	
CF	1	75.54	71.85	5.1	5.3
	2	79.50	75.54	5.2	
	3	78.19	74.13	5.5	
BMR	1	56.70	54.34	4.3	4.1
	2	47.32	45.4	4.2	
	3	47.33	45.61	3.8	
BCR	1	56.65	54.49	4.0	3.9
	2	55.8	53.73	3.9	
	3	51.6	49.68	3.9	
#12FM	1	85.32	82.29	3.7	3.5
	2	66.57	64.22	3.7	
	3	72.89	70.71	3.1	
#12FC	1	80.22	76.22	5.2	5.1
	2	79.58	75.49	5.4	
	3	75.24	71.93	4.6	

Table 4 Notes:

CR: Roof specimen, cyclic loading

CF: Floor specimen, cyclic loading

BMR: Roof specimen blocked, monotonic loading

BCR: Roof specimen blocked, cyclic loading

#12FM: Floor specimen with #12 screws, monotonic loading

#12FC: Floor specimen with #12 screws, cyclic loading

8- Diaphragm Experimental Results

8.1 Part 1 Diaphragm Tests

8.1.1 Loading Protocol

The diaphragm specimens were tested under monotonic and reversed cyclic displacement based loading. The CUREE loading protocol (Krawinkler et al. 2000) was followed for the cyclic loading to be consistent with that used for the many CFS framed wall tests at McGill University. As explained in Section 4 of this report, first a reference displacement was obtained from the monotonic test, which was multiplied by a 0.6 reduction factor to account for the earlier deterioration in strength expected in the cyclic test compared to the monotonic one. This reference displacement is then used to create a loading protocol involving initiation, primary and trailing cycles. For example, Table 5 indicates the loading protocol of the No.2 diaphragm specimen, while Figure 14 provides an illustration of these displacements versus time.

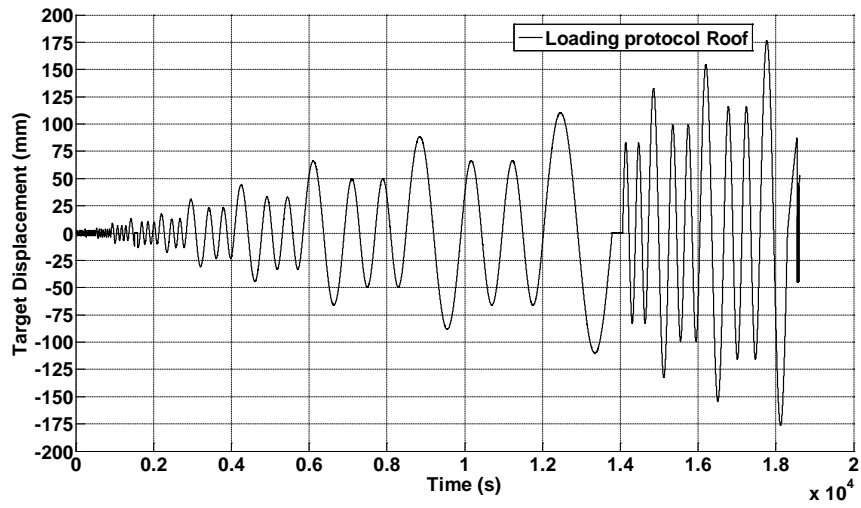


Figure 14: Reversed cyclic loading protocol of roof configuration

Table 5: Reversed cyclic loading protocol of roof configuration

Amplitudes of cycles		Target Displacement (mm)	Number of Cycles
0.05	Δ	2.2	6
0.075	Δ	3.3	1
0.056	Δ	2.5	6
0.1	Δ	4.4	1
0.075	Δ	3.3	6
0.2	Δ	8.8	1
0.15	Δ	6.6	3
0.3	Δ	13.2	1
0.225	Δ	9.9	3
0.4	Δ	17.7	1
0.3	Δ	13.2	2
0.7	Δ	30.9	1
0.525	Δ	23.2	2
1	Δ	44.2	1
0.75	Δ	33.1	2
1.5	Δ	66.2	1
1.125	Δ	49.7	2
2	Δ	88.3	1
1.5	Δ	66.2	2
2.5	Δ	110.4	1
1.875	Δ	82.8	2
3	Δ	132.5	1
2.25	Δ	99.3	2
3.5	Δ	154.5	1
0.2625	Δ	11.6	2
4	Δ	176.6	1

The rate of the displacement applied for the Part 1 monotonic tests was 2.5mm/min for the roof and 5mm/min for the floor configuration, while for the cyclic tests the displacement rate started with 15mm/min and after a displacement of approximately 60mm was increased to 60mm/min.

8.1.2 Test Results

Initially, the bare steel framing without the sheathing panels was tested under monotonic loading (remaining in the elastic region, Figure 15 for specimens No. 1 and 2).

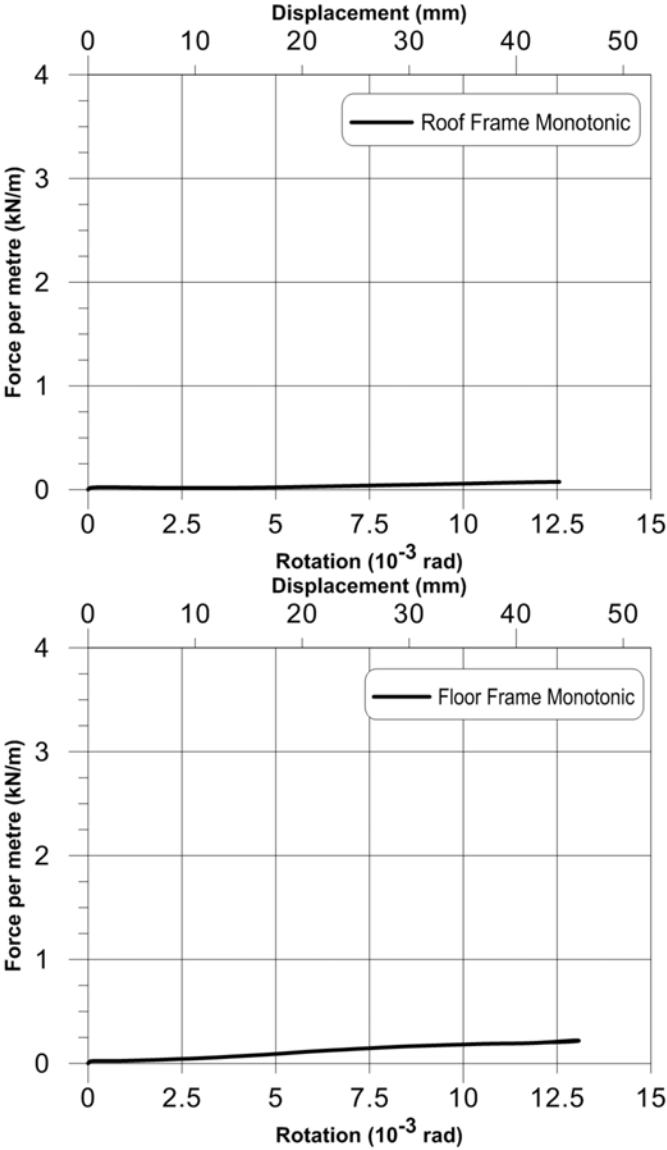


Figure 15: Shear force vs. rotation response for the bare steel frame of diaphragm roof and floor configurations No. 1 & 2

It is shown that the contribution to shear strength and stiffness of the bare steel frame was negligible.

Figures 16 and 17a, b demonstrate the monotonic and reversed cyclic results obtained for specimens No. 3 and 4 and the deformation experienced by the diaphragm specimen during the tests. Figures 18 and 19a, b include the corresponding results for specimens No. 5 and 6. A summary of all the shear resistances of the diaphragms tested is presented in Table 6 at the end of Section 8. The cyclic degradation behaviour is evident in the shear force vs. rotation response for each specimen presented herein.

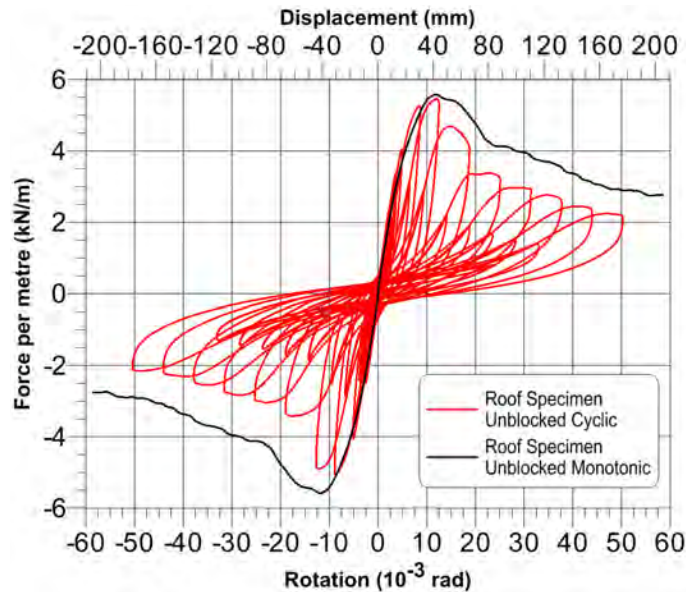
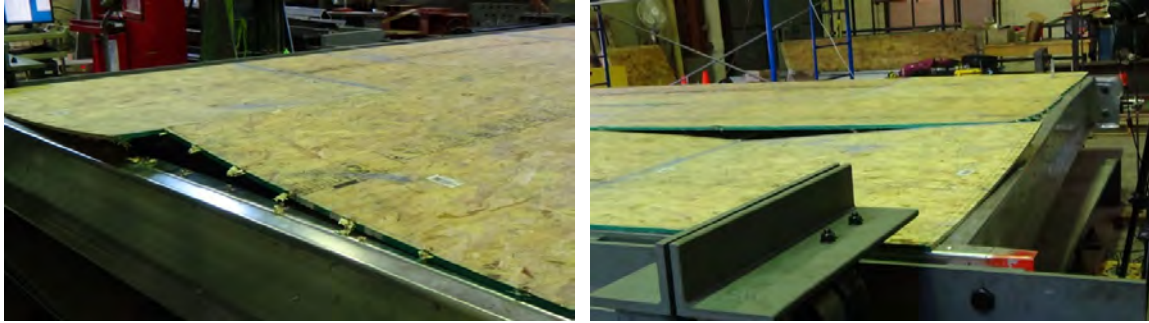


Figure 16: Shear force vs. rotation response for Part 1 diaphragm roof specimens No. 3 & 4

Figure 16 contains graphs showing the shear force vs. rotation (deformation) response of the two roof diaphragm specimens. The cyclic and monotonic specimens behaved similarly with screws tearing out or pulling through the wood after wood bearing had occurred. Failure was concentrated in the middle row of the panels where fewer screws were used since this is the case of an unblocked diaphragm (304mm (12in) o/c spacing). Lift off of panels was observed in these intermediate locations as illustrated in Figures 17a and 17b.



(a) Deformation from monotonic loading



(b) Deformation from cyclic loading

Figure 17: Deformation for Part 1 diaphragm roof specimens No. 3 & 4

Figure 18 contains graphs showing the shear force vs. rotation (deformation) response of the two floor diaphragm specimens. A steeper decline in shear strength was measured after the maximum load had been reached compared with the roof diaphragm specimens. The screws remained vertical and the failure mode involved primarily shear fracture of the #10 sheathing screws, although some edge bearing damage to the OSB was also observed. In addition, there was an

increase in shear strength observed towards the end of the monotonic test, i.e. after 35 mrad, while the final excursions of the cyclic test showed that the load was being maintained. This effect was attributed to the contact/bearing (friction) action between the edges of the OSB panels which occurred after most of the sheathing screws had failed in shear. There was no lift off of panels in this configuration due to the tongue & groove (T&G) characteristic of the wood panels, which aided in the development of this contact resistance, as shown in Figure 19. Note, the maximum displacement of the reversed cyclic test was less than that of the monotonic due to limitations of the actuator stroke.

Based on the results shown in Figures 16, 17, 18 and 19 the floor configuration exhibited higher shear strength but experienced a more rapid post-peak decrease in strength compared with the roof configuration. There was a gradual increase in the shear strength after 35 mrad, observed mostly in the monotonic test, due to the T&G characteristic of the floor configuration panels that was not present for the roof configuration. It is shown that the T&G panels led to a constant level of shear strength being maintained at large displacements and ensured the connectivity between the panels even after the diaphragm was damaged, which led to safer working conditions (walking on top of the diaphragm before and after testing); thus, their implementation as a design detail for the roof configuration as well should be considered.

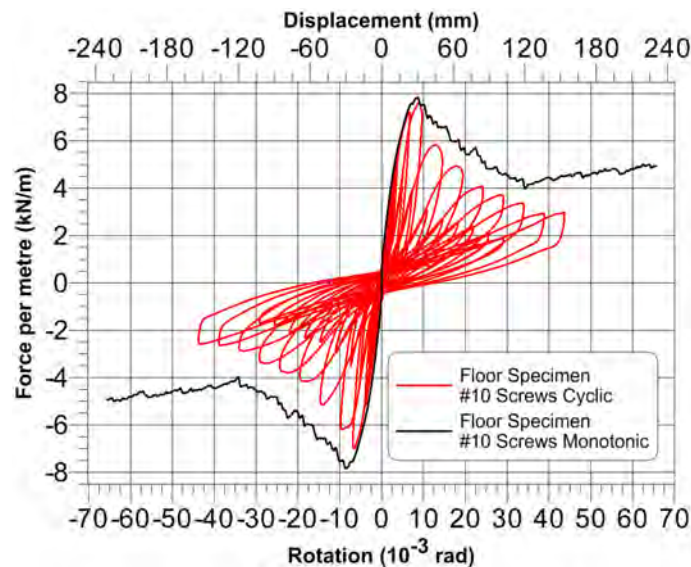


Figure 18: Shear force vs. rotation response for Part 1 diaphragm floor specimens No. 5 & 6



(a) Deformation from monotonic loading



(b) Deformation from cyclic loading

Figure 19: Deformation for Part 1 diaphragm roof specimens No. 3 & 4

8.2 Part 2 Diaphragm Tests

As explained in Section 5.2.2, it was decided, based on the results presented in Section 8.1 for Part 1 of the experimental program, that the same configurations would be tested under monotonic and reversed cyclic loading with the roof diaphragm specimens (No. 7 & 8) being fully blocked (full height blocking) and the floor diaphragm specimens (No. 9 & 10) being assembled using #12 sheathing screws instead of #10. A fully blocked case was chosen for the roof configuration so as to investigate the effect of fully supporting and fastening all edges of the OSB panels. This approach was taken given that in the Phase 1 tests (No. 3 & 4) the failures occurred along the edges of the intermediate panels, which were not fully connected to the underlying steel framing. For the floor configuration, #12 screws were used in order to investigate the effect of the size of the screw on the diaphragm's strength and stiffness given that

the failure mode observed in Phase 1 involved mainly shearing of the sheathing screws. Figures 20 and 22 contain graphs showing the shear force vs. rotation (deformation) response of the Phase 2 roof and floor diaphragm specimens. Figures 21a, b and 23 show photographs that illustrate the failure modes observed for these modified diaphragm configurations.

In Figure 20 it is shown that by adding the extra blocking and screws around the perimeter of each panel (152 mm (6in) o/c spacing) the maximum load was reached (Table 6) after which a quick loss of strength followed. The fasteners were tilting, shearing and pulling through the OSB near the fixed connection of the diaphragm to the frame (Figure 21). In this location there were fewer screws because of the 152mm (6in) wood panel extending inside the connection, as explained in Section 5.2.1. Effectively, the width of the panels at this side of the diaphragm was 152 mm shorter than all other panels, and as such these panels represented the weakest section of the test specimen. Once the sheathing connections in these edge panels had failed the force transferring through the diaphragm assembly had to pass through the underlying steel framing by means of bending action, i.e. there was no diaphragm action in that location (Figure 21a).

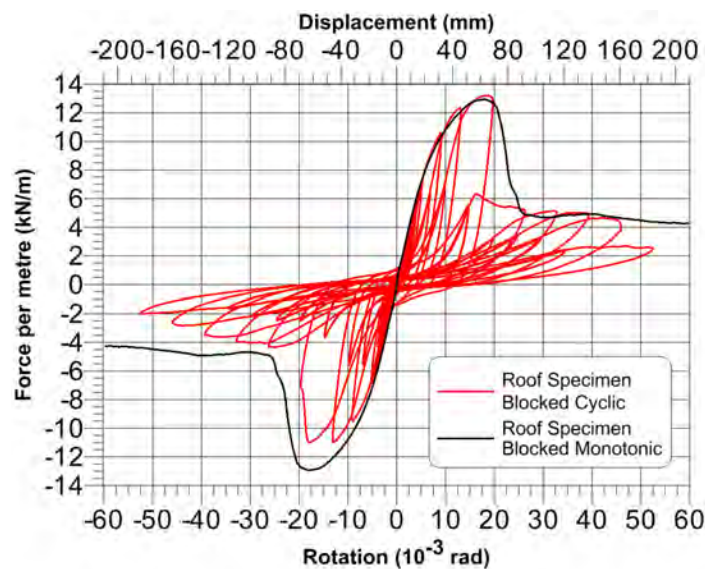
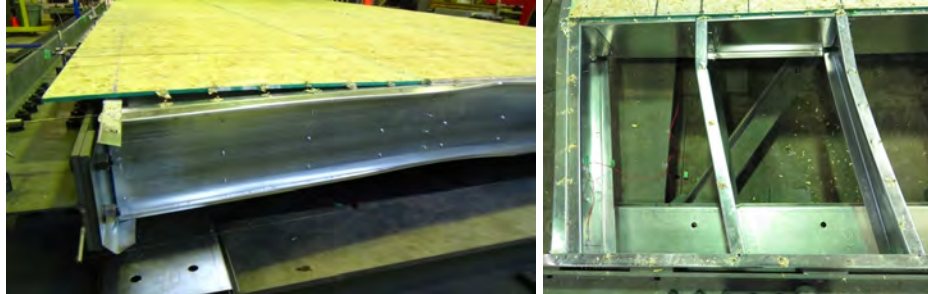


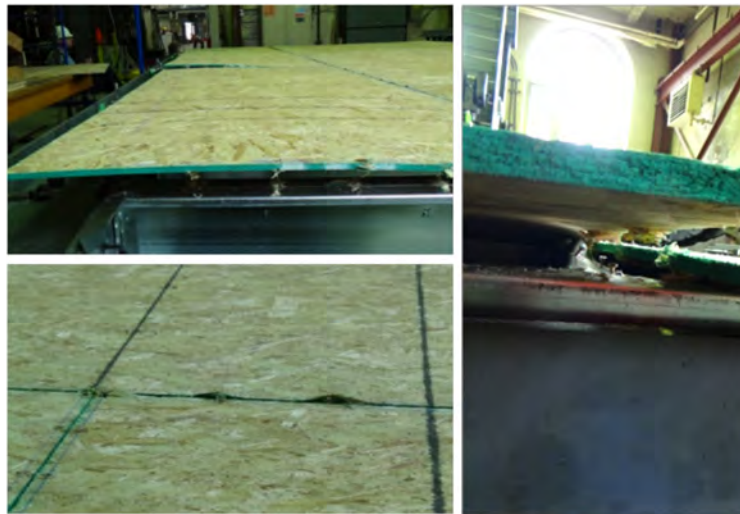
Figure 20: Shear force vs. rotation response for Part 2 diaphragm roof specimens No. 7 & 8

It is this frame action of the CFS framing that resulted in the load stabilizing into a constant value, as observed in the monotonic and reversed cyclic shear force vs. rotation curves (Figure 20). The damage to the sheathing connections also extended to the middle OSB panels.

Furthermore, there was shearing of the perimeter screws mostly in the double steel locations (rim joist - joist - sheathing). The specimen behaved similarly for the reversed cyclic and monotonic loading.



(a) Deformation from monotonic loading



(b) Deformation from cyclic loading

Figure 21: Deformation for Part 2 diaphragm roof specimens No. 7 & 8

For the floor configuration with #12 sheathing screws the specimens (No. 9 & 10) exhibited an effective redistribution of forces and all sheathing screws contributing throughout the loading protocol, as indicated in Figure 22. A combination of shear and tensile forces was applied to the screws as the wood panels lifted up from the framing along their edges resulting in the screws tilting before shearing or pulling out the steel (Figure 23). In some locations wood panel edge contact/bearing (friction) action took place after the pull out or shearing of screws stabilizing the

load towards the end of the test. Steel – to – steel shearing of some screws was also observed and the joist flanges were distorted due to the applied shear and uplift forces from the sheathing.

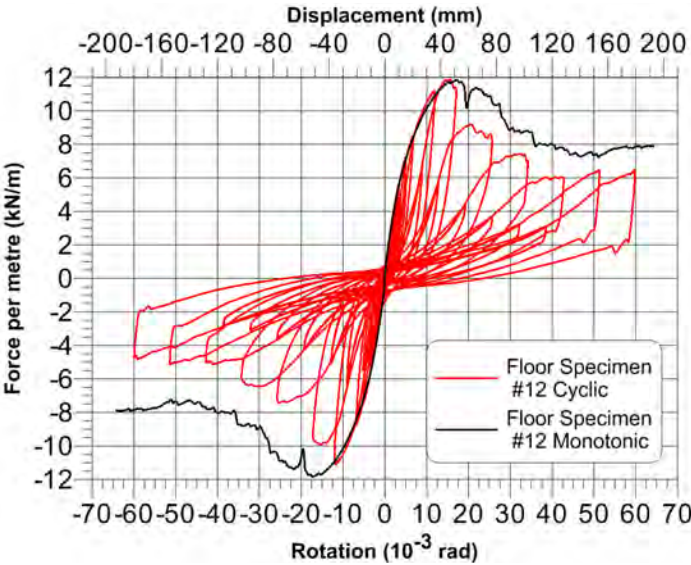
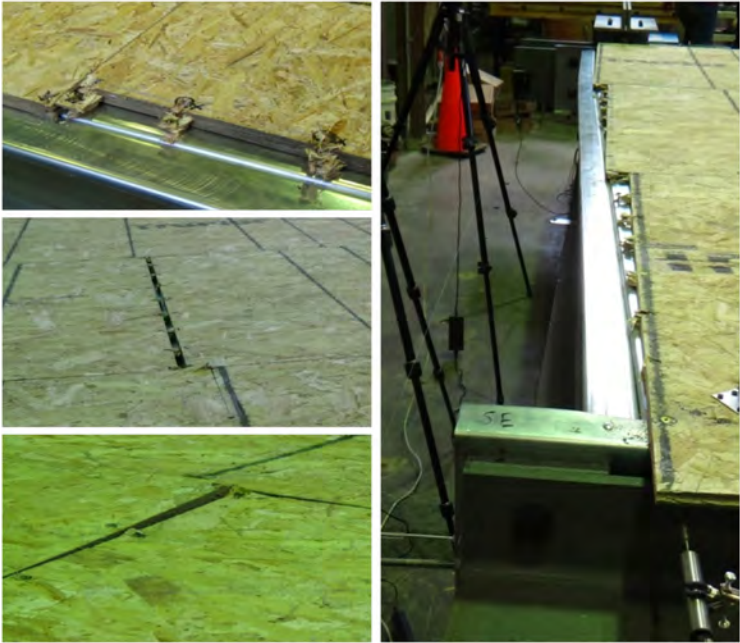


Figure 22: Shear force vs. rotation response for Part 2 diaphragm roof specimens No. 9 & 10



(a) Diaphragm behaviour from monotonic loading

Figure 23: Deformation for Part 2 diaphragm roof specimens No. 9 & 10



(b) Diaphragm behaviour from cyclic loading

Figure 23 (Continued): Deformation for Part 2 diaphragm roof specimens No. 9 & 10

8.3 Comparison of Part 1 and Part 2 Diaphragm Response to Loading

A comparison between the No. 3 & 4 (Part 1) and No. 7 & 8 (Part 2) diaphragm specimens (unblocked vs. blocked case) is provided in Figure 24.

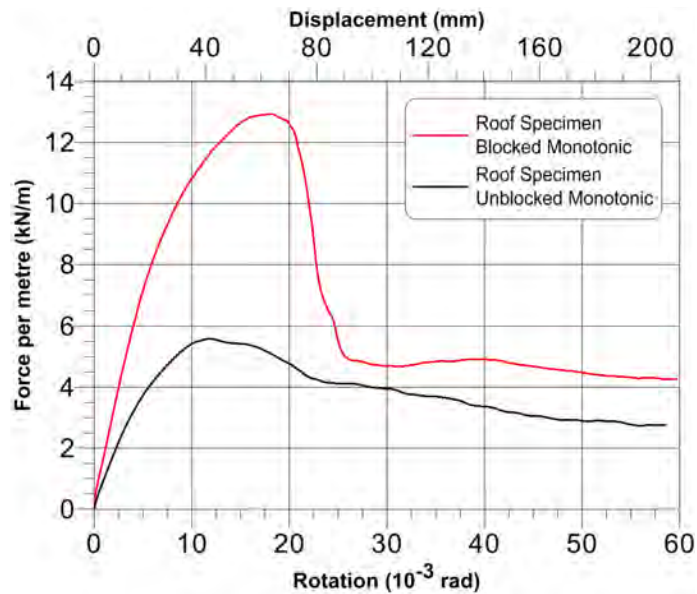


Figure 24: Shear force vs. rotation response for fully blocked versus unblocked roof diaphragm

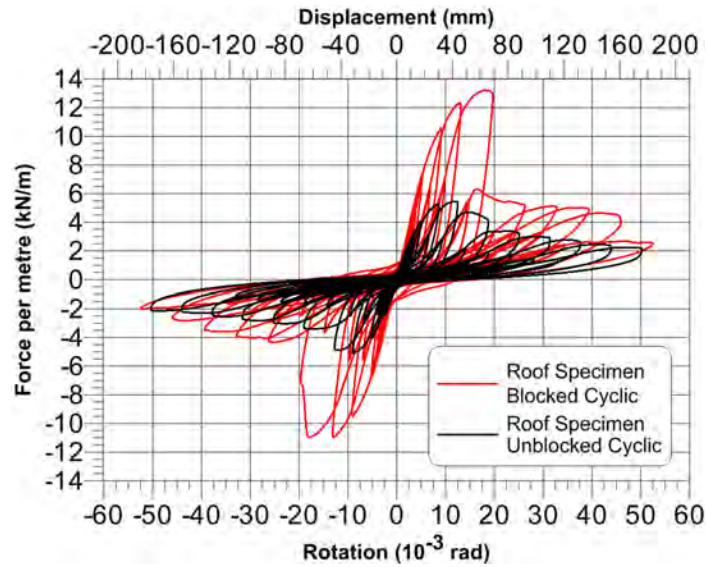


Figure 24 (Continued): Shear force vs. rotation response for fully blocked versus unblocked roof diaphragm

It is shown that there was an increase of 130% in shear resistance and 70% in shear stiffness by adding the extra blocking and the extra screws along the perimeter of the OSB panels (152 mm (6in) o/c spacing). Although the ultimate resistance was higher in the Part 2 tests, the shear resistance decreased suddenly in the post peak range due to the failure of the sheathing connections in the row of panels along the fixed edge of the test-setup as described in Section 8.2. However, it should be noted that in typical construction the presence of a wall connected to the 152 mm extension of the OSB diaphragm panels would likely have reinforced the edge of the test specimen and shifted the location where failure was concentrated to the central portion of the diaphragm. Furthermore, given that the sheathing connections of the interior OSB panels were near failure at the end of the test, it is hypothesized that the ultimate shear resistance of the Part 2 roof specimens if attached to a wall would not have shown a substantial increase from that which was measured. A comparison was realised for the No. 5 & 6 (Part 1) and No. 9 & 10 (Part 2) diaphragm specimens (#10 vs. #12 screws) as shown in Figure 25.

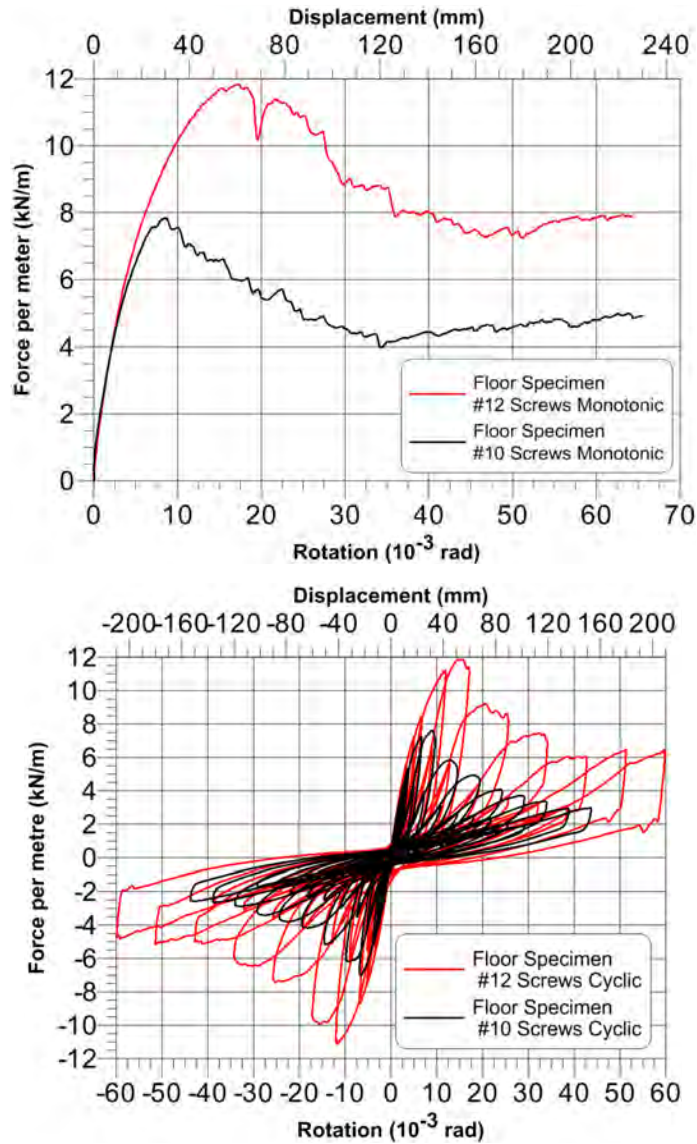


Figure 25: Shear force vs. rotation response for #12 versus #10 sheathing screws floor diaphragm

A 50% increase in shear resistance was observed due to the change of the screw size. The No.9 & 10 diaphragm specimens exhibited a better redistribution of forces, observed through a survey of the sheathing connection damage, and some screws continued to contribute while the panel edge bearing action commenced. Moreover, the failure mode of the diaphragm changed. The use of the #12 screws led to wood bearing damaged of the OSB panels instead of the sudden fastener shear failures observed for the Part 1 diaphragm specimens with #10 screws. However, both specimens exhibited similar decrease in shear resistance after the peak load was reached (Figure

25). Table 6 summarizes the shear resistances of the specimens. Information about the deflection is provided in Section 9.

Table 6: Summary of shear resistance results

Diaphragm Specimens	Part 1		Part 2	
	No.3 & 4 (roof unblocked)	No.5 & 6 (floor #10 screws)	No.7 & 8 (roof blocked)	No.9 & 10 (floor #12screws)
Shear Resistance, v (kN/m)	5.59	7.83	12.93	11.84

9- Design Predictions

This section contains a description of the procedure for calculating design deflection and shear resistance values for CFS framed diaphragms based on the AISI S213 Standard (2007). Note, this existing design procedure for diaphragms will be carried forward to the new AISI S400 Standard (2015).

9.1 Deflection

In order to predict the in-plane deflection of a blocked CFS framed - wood sheathed cantilever diaphragm, Equation C2.1.1 (AISI S213 2007) or E1.4.1.4-1 (AISI S400 2015) (Equation 1.2 in this document), which is intended for cantilever shear walls, was utilized:

$$\delta = \frac{2vh^3}{3E_s A_c b} + \frac{\omega_1 \omega_2 v h}{\rho G t_{sheathing}} + \omega_1^4 \omega_2 \omega_3 \omega_4 \left(\frac{v}{\beta}\right)^2 + \frac{h}{b} \delta_v, \text{ where} \quad (1.2)$$

A_c = Gross cross-sectional area of chord member, in square inches (mm^2)

b = Width of the shear wall, in inches (mm)

E_s = Modulus of elasticity of steel 29,500 ksi (203,000 MPa)

G = Shear modulus of sheathing material, in pounds per square inch (MPa)

h = Wall height, in inches (mm)

s= Maximum fastener spacing at panel edges, in inches (mm)

$t_{\text{sheathing}}$ = Nominal panel thickness, in inches (mm)

t_{stud} = Nominal framing thickness, in inches (mm)

v= Shear demand (V/b), in pounds per linear inch (N/mm)

V = Total in-plane load applied to the diaphragm, in pounds (N)

β = 67.5 for plywood and 55 for OSB for U.S. Customary (lb/in^{1.5})
2.35 for plywood and 1.91 for OSB for SI units (N/mm^{1.5})

δ = Calculated deflection, in inches (mm)

δ_v = Vertical deformation of anchorage / attachment details, in inches (mm)

ρ = 1.85 for plywood and 1.05 for OSB

ω_1 = s/6 (for s in inches)

= s/152.4 (for s in mm)

ω_2 = 0.033/ t_{stud} (for t_{stud} in inches)

= 0.838/ t_{stud} (for t_{stud} in mm)

$$\omega_3 = \sqrt{\frac{h}{2b}}$$

ω_4 = 1 for wood with structural panels

Equation 1.2 was deemed appropriate for use because a cantilever test configuration was used, in contrast to the assumed simply supported diaphragm configuration deflection equation found in AISI S213 and the commentary of AISI S400. Note; comparison with the diaphragm deflection estimates based on the simply supported configuration are provided at the end of this Section. A prediction of the vertical deformation of anchorage, δ_v , used in Equation 1.2 is not available. Hence, the value used in the prediction was obtained from the maximum measurement taken during each respective test. Table 7 contains a comparison of the results generated from Equation

1.2 (cantilever configuration) to the measured displacement at ultimate load as observed during testing.

Table 7: Comparison of measured displacement at ultimate load versus calculated deflection using Equation 1.2 with δ_v maximum

Diaphragm Specimens	Part 1		Part 2	
	No.3 & 4 (roof unblocked)	No.5 & 6 (floor #10 screws)	No.7 & 8 (roof blocked)	No.9 & 10 (floor #12 screws)
δ_{Test} (mm)	41.3	29.8	63.1	60.7
$\delta_{Calculated}$ AISI (mm)	10.1	9.0	29.5	17.3
% Error	75.5	69.7	53.2 ⁽¹⁾	71.5

⁽¹⁾ Equation 1.2 is based on shear walls which are assumed to be blocked, this could be the reason the error is reduced for this case. In the AISI S213 Standard (2007) for unblocked diaphragms an unblocked factor of 2.5 is incorporated. However, no such factor exists for the shear wall deflection calculations.

Sample Calculation

Deflection calculation using Eq. 1.2 for No.1 diaphragm specimen

$$A_c = 1230 \text{ mm}^2 \text{ (2x 1200S200-54)}$$

$$b = 6096 \text{ mm (20ft)}$$

$$E_s = 203000 \text{ MPa}$$

$$G = \frac{G_v t_v}{t_{sheathing}} = \left(\frac{14629 \left(\frac{N}{mm} \right)}{11.11 mm} \right) = 1317 \text{ N/mm}^2 \text{ (24/16 rating OSB)}$$

the shear modulus, G, is not a readily available value in most cases. Here G is approximated by dividing the through thickness shear rigidity ($G_v t_v$) by the nominal panel thickness ($t_{sheathing}$). The through thickness shear rigidity ($G_v t_v$) is taken from Table A (Figure 26), which was obtained from TECO's document entitled *Design Capacities for Oriented Strand Board* (TECO, 2008). These values correspond with those published in the 2005 edition of the AF&PA American Wood Council's *Allowable Stress Design (ASD)/LRFD Manual for Engineered Wood Construction*. It is important to note that the construction adjustment factor C_G was incorporated into the design values found in Table A (Figure 26).

Table A
Wood Structural Panel Design Capacities Based on Span Ratings^(a)

Span Rating	Strength							Planar Shear	Stiffness and Rigidity				
	Bending F _b S (lb-in/ft of width)		Axial Tension F _t A (lb/ft of width)	Axial Compression F _c A (lb/ft of width)		Shear through the thickness ^(b) F _v t _v (lb/in of shear-resisting panel length)	Planar Shear F _s (lb/Q) (lb/ft of width)	Bending EI (lb-in ² /ft of width)	Axial ^(a1) EA (lb/ft of width x 10 ⁶)	Rigidity through the thickness G _v t _v (lb/in of panel depth)			
	Capacities relative to strength axis ^(c)												
	0°	90°	0°	90°	0°	90°	0° / 90°	0° / 90°	0°	90°	0°	90°	0° / 90°
Sheathing Span[®]													
24/0	300	97	2,300	780	2,850	2,500	155	130	60,000	11,000	3.35	2.50	77,500
24/16	385	115	2,600	1,300	3,250	2,500	165	150	78,000	16,000	3.80	2.70	83,500
32/16	445	165	2,800	1,650	3,550	3,100	180	165	115,000	25,000	4.15	2.70	83,500
40/20	750	270	2,900	2,100	4,200	4,000	195	205	225,000	56,000	5.00	2.90	88,500
48/24	1,000	405	4,000	2,550	5,000	4,300	220	250	400,000	91,500	5.85	3.30	96,000
Floor Span[®]													
16 oc	500	180	2,600	1,900	4,000	3,600	170	205	150,000	34,000	4.50	2.70	83,500
20 oc	575	250	2,900	2,100	4,200	4,000	195	205	210,000	40,500	5.00	2.90	87,000
24 oc	770	385	3,350	2,550	5,000	4,300	215	250	300,000	80,500	5.85	3.30	93,000
32 oc	1,050	685	4,000	3,250	6,300	6,200	230	300	650,000	235,000	7.50	4.20	110,000
48 oc	1,900	1,200	5,600	4,750	8,100	6,750	305	385	1,150,000	495,000	8.20	4.60	155,000

- (a) The design values in this table correspond with those published in the 2005 edition of the AF&PA American Wood Council's *Allowable Stress Design (ASD)/LRFD Manual for Engineered Wood Construction* Tables M9.2.1- M9.2.4, which are available from the AF&PA American Wood Council.
- (a1) In late January 2008, revised Axial EA 90° (perpendicular) values were submitted for modification to AF&PA based on an industry-wide consensus. The appropriate panel grade and construction adjustment factor, C_o, has already been incorporated into these design values—do not apply the C_o factor a second time. These values do not apply to Structural I panels. See Tables M9.2.1 – M9.2.4 for the appropriate multipliers for Structural I panels.
- (b) Shear through the thickness design capacities are limited to sections two feet or less in width; wider sections may require further reductions.
- (c) Strength axis is defined as the axis parallel to the face and back orientation of the flakes, which is generally the long panel direction, unless otherwise marked.

Figure 26: Table A used to find G_vt_v in order to approximate shear modulus, G (TECO, 2008).

As a reference value the shear modulus calculated from the Canadian Standards Association (CSA) O86 Standard Table 7.3C (CSA 2009) assuming a thickness of 11.11 mm, short term loading (K_D = 1.15) and a 1R24/2F16 OSB performance rating gives a value of G = 1139 N/mm². The previously calculated value (G = 1317 N/mm²) is used as it is the value suggested by the OSB provider Norbord based on the testing of their products.

$$h = 3505 \text{ mm}$$

$$s = 152.4 \text{ mm (6in)}$$

$$t_{\text{sheathing}} = 11.11 \text{ mm (7/16in OSB)}$$

$$t_{\text{stud}} = 1.438 \text{ mm (1200S200-54)}$$

$$v = V/b = \frac{34083 \text{ N}}{6096 \text{ mm}} = 5.59 \text{ N/mm}$$

$$V = 34083 \text{ N}$$

$$\beta = 1.91 \text{ N/mm}^{1.5} \text{ (Standard OSB)}$$

$$\rho = 1.05 \text{ (Standard OSB)}$$

$$\delta_v = 11.48 \text{ mm (based on maximum measured value from test)}$$

$$\omega_1 = s/152.4 = 152.4\text{mm}/152.4 = 1.0$$

$$\omega_2 = 0.838/ t_{\text{stud}} = 0.838/1.438\text{mm} = 0.583$$

$$\omega_3 = \sqrt{\left(\frac{h}{b}\right)/2} = \sqrt{\left(\frac{7010}{6096}\right)/2} = 0.758$$

$$\omega_4 = 1 \text{ (wood structural panels)}$$

$$\begin{aligned} \delta &= \frac{2vh^3}{E_s A_c b} + \frac{\omega_1 \omega_2 v h}{\rho G t_{\text{sheathing}}} + \omega_1^{\frac{5}{4}} \omega_2 \omega_3 \omega_4 \left(\frac{v}{\beta}\right)^2 + \frac{h}{b} \delta_v \\ &= \frac{2 \left(\frac{5.59\text{N}}{\text{mm}}\right) (3505\text{mm})^3}{203000\text{Mpa}(1230\text{mm}^2)(6096\text{mm})} + 1\text{mm} * 0.583\text{mm} \\ &\quad * \frac{\left(\frac{5.59\text{N}}{\text{mm}}\right) (3505\text{mm})}{1.05 \left(\frac{1317\text{N}}{\text{mm}^2}\right) (11.11\text{mm})} + 1.0^{\frac{5}{4}} * 0.583 * 0.758 * 1.0 \left(\frac{\frac{5.59\text{N}}{\text{mm}}}{\frac{1.91\text{N}}{\text{mm}^{1.5}}}\right)^2 \\ &\quad + \left(\frac{3505\text{mm}}{6096\text{mm}}\right) * 11.48\text{mm} = 10.13\text{mm} \end{aligned}$$

$$\% \text{ Error} = \frac{|\delta_{\text{observed}} - \delta_{\text{calculated}}|}{\delta_{\text{observed}}} * 100 = \frac{|41.3 - 10.13|}{41.3} * 100\% = 75.5\%$$

In order to obtain an alternate deflection value for comparison purposes, the displacement at the intercept of the initial linear elastic stiffness, δ_{ELASTIC} , and ultimate load of each specimen was obtained from the test results, as shown in Figure 27. The δ_{ELASTIC} was based on the maximum deflection assuming an elastic system using the in-plane lateral elastic stiffness, K_e . The results of this process are summarised in Table 8.

K_e is calculated based on Equation 1.3:

$$K_e = \frac{v_{0.4}}{\Delta_{0.4v}}, \text{ where} \quad (1.3)$$

$v_{0.4}$ = 40% of the peak shear demand per metre S_u

$\Delta_{0.4v}$ = in-plane lateral displacement of the wall corresponding to $v_{0.4}$

$\delta_{ELASTIC}$ can then be calculated by Equation 1.4:

$$\delta_{ELASTIC} = \frac{v}{K_e}, \text{ where} \quad (1.4)$$

v = Peak shear demand

K_e = Elastic stiffness

Sample Calculation

Equivalent elastic deflection calculation for Part 1 roof diaphragm (unblocked, monotonic)

$v_{0.4} = 2.24 \text{ kN/mm}$

$\Delta_{0.4v} = 8.97 \text{ mm}$

$$K_e = \frac{\frac{2.24 \text{ kN}}{\text{mm}}}{8.97 \text{ mm}} = \frac{0.250 \text{ kN}}{\text{mm}^2}$$

$v = 5.59 \text{ kN/mm}$

$K_e = 0.250 \text{ kN/mm}^2$

$$\delta_{ELASTIC} = \frac{\frac{5.59 \text{ kN}}{\text{mm}}}{\frac{0.250 \text{ kN}}{\text{mm}^2}} = 22.36 \text{ mm}$$

Table 8: Comparison of displacement based on initial linear elastic stiffness versus calculated deflection using Equation 1.2 with δ_v elastic

Diaphragm Specimens	Part 1		Part 2	
	No.3 & 4 (roof unblocked)	No.5 & 6 (floor #10 screws)	No.7 & 8 (roof blocked)	No.9 & 10 (floor #12 screws)
$\delta_{Elastic}$ (mm)	22.4	13.2	29.5	23.5
$\delta_{Calculated}$ (mm) ⁽¹⁾	10.0	8.35	29.4	14.4
% Error	55.4	36.7	0.0	38.7

(1) The deflection calculation uses the maximum δ_v in the elastic region

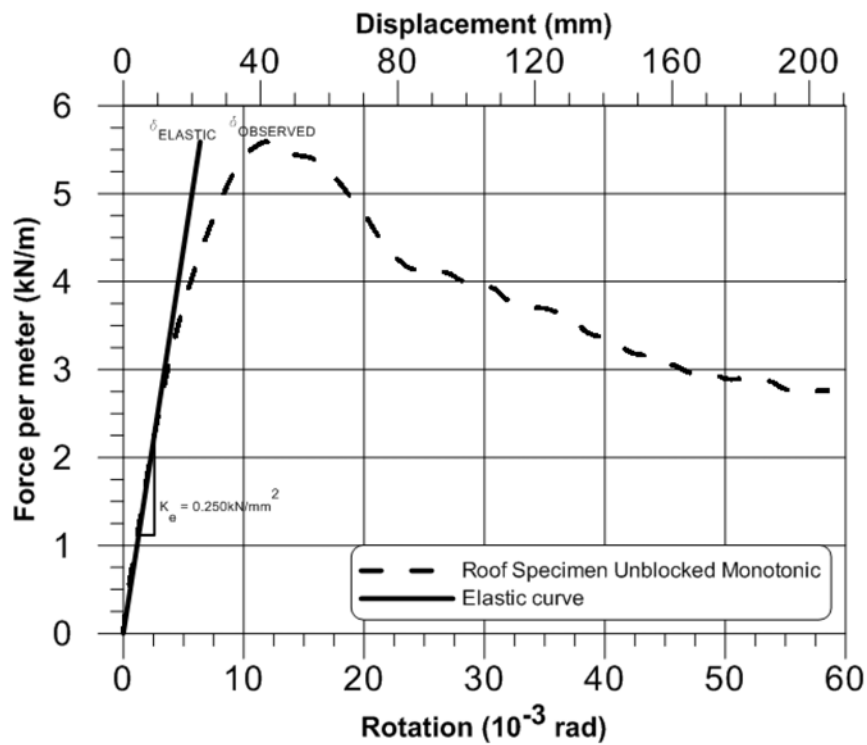


Figure 27: Elastic deflection as obtained from elastic shear force vs. rotation curve

The calculated displacement listed in Table 8 differed from that provided in Table 7 due to the δ_v value being that measured during the elastic range of loading. For example, in the example calculation shown previously for the No.1 diaphragm specimen, the value of δ_v was taken as

11.48 mm, whereas for the prediction listed in Table 8 δ_v was 11.25 mm. The results in Table 8 indicate that focusing on the elastic response of the diaphragm reduces the error between the calculated and experimental displacement. It should be noted that for the unblocked configurations (No. 3, 4, 5, 6, 9 & 10) the error would be reduced if an amplification factor were to be implemented. The 2.5 factor suggested for the diaphragm deflection equation (Eq. D2.1 AISI S213 2007 / Eq. C-F2.4.3-1 AISI S400 2015) is based on experimental data of simply supported wood diaphragm configurations (APA 2007); thus, its application is questionable for the data presented herein given the change in loading configuration. The calculated and measured elastic deflection values for the blocked diaphragm configuration (No. 7 and 8) are in good agreement.

Overall, the lack of conformity between the measured and calculated deflection values is attributed to the fact that Eq. 1.2 as described in this report is based on experimental work of 1220 mm x 2440 mm (4' x 8') shear walls (Serrette and Chau 2003). The behaviour of which is different from that observed for the diaphragm specimens presented herein. As described in Section 8, the diaphragm behaviour was governed by a sharp drop of strength after the peak load was reached and had characteristics such as joist bending and bearing or lift-off of panels in the intermediate panel locations; this behaviour does not comply with the gradual yielding exhibited by the fully blocked one panel shear walls referred to in Serrette and Chau (2003). The multiple panels used in a diaphragm, gaps between panel edges and the possibility of having unfastened sections of panel edges, where unblocked, leads to much larger measured displacement values than anticipated.

The following comparison was realised between the deflection values for each diaphragm configuration calculated using Eq. D2.1 of AISI S213 (2007) (Eq. C-F2.4.3-1 of AISI S400 (2015)) (Eq. 1.3 in this report) for simply supported diaphragms (Table 9) and the measured $\delta_{Elastic}$. It is illustrated that the error between the calculated and the measured data is considerably increased in this case. The 2.5 factor for the unblocked diaphragm is included in the results shown. It should be noted that given there were no chord splices in the test configurations the last term of Eq. 1.3 was neglected.

$$\delta = \frac{0.052vL^3}{E_s A_c b} + \frac{\omega_1 \omega_2 v L}{\rho G t_{sheathing}} + \omega_1^4 \omega_2 (\alpha) \left(\frac{v}{2\beta} \right)^2 + \frac{\sum_{j=1}^n \Delta_{ci} X_i}{2b}, \text{ where} \quad (1.3)$$

A_c = Gross cross-sectional area of chord member, in square inches (mm²)

b = Diaphragm depth parallel to direction of load, in inches (mm)

E_s = Modulus of elasticity of steel 29,500,000 psi (203,000 MPa)

G = Shear modulus of sheathing material, in pounds per square inch (Mpa)

L = Diaphragm length perpendicular to direction of load, in inches (mm)

N = Number of chord splices in diaphragm (considering both diaphragm chords)

S = Maximum fastener spacing at panel edges, in inches (mm)

$t_{sheathing}$ = Nominal panel thickness, in inches (mm)

t_{stud} = Nominal framing thickness, in inches (mm)

v = Shear demand ($V/2b$), in pounds per linear inch (N/mm)

V = Total lateral load applied to the diaphragm, in pounds (N)

X_i = Distance between the “ith” chord-splice and the nearest support (braced wall line), in inches (mm)

α = Ratio of the average load per fastener based on a non-uniform fastener pattern to the average load per fastener based on a uniform fastener pattern (= 1 for a uniformly fastened diaphragm)

β = 67.5 for plywood and 55 for OSB for U.S. Customary (lb/in^{1.5})

2.35 for plywood and 1.91 for OSB for SI units (N/mm^{1.5})

δ = Calculated deflection, in inches (mm)

Δ_{ci} = Deformation value associated with “ith” chord splice, in inches (mm)

ρ = 1.85 for plywood and 1.05 for OSB

ω_1 = $s/6$ (for s in inches)

= $s/152.4$ (for s in mm)

ω_2 = $0.033/t_{stud}$ (for t_{stud} in inches)

= $0.838/t_{stud}$ (for t_{stud} in mm)

For unblocked diaphragms, δ shall be multiplied by 2.50.

Table 9: Comparison of displacement based on initial linear elastic stiffness versus calculated deflection using Equation 1.3

Diaphragm Specimens	Part 1		Part 2	
	No.3 & 4 (roof unblocked)	No.5 & 6 (floor #10 screws)	No.7 & 8 (roof blocked)	No.9 & 10 (floor #12 screws)
δ_{Elastic} (mm)	22.4	13.2	29.5	23.5
$\delta_{\text{Calculated}}$ (mm)	7.0	6.1	10.3	11.8
% Error	68.8	53.8	65.1	49.8

9.2 Shear Resistance

In order to predict the design shear resistance of the diaphragms Table D2-1 was used from the AISI S213 Standard (2007), as shown in Figure 27. The same table is included in the new AISI S400 Standard (2015) as Table F2.4-1. Table 10 lists the nominal shear strength values for each diaphragm configuration.

Table 10: Comparison of measured and nominal shear resistance

Diaphragm Specimens	Part 1		Part 2	
	No.3 & 4 (roof unblocked)	No.5 & 6 ⁽¹⁾ (floor #10 screws)	No.7 & 8 (roof blocked)	No.9 & 10 ⁽¹⁾ (floor #12screws)
Shear Strength (lbs/ft)	505	555	760	555
Shear Strength (kN/m)	7.37	8.10	11.10	8.10
Peak Load During Tests (kN/m)	5.59	7.83	12.93	11.84

(1) Due to lack of data, the diaphragm values included in Table 10 for diaphragm specimens No.5, 6, 9 and 10 (floor configuration) correspond to 15/32in OSB thickness when in reality 23/32in OSB panels were used. Further, diaphragm configurations fastened with #12 screws are not listed in AISI S213.

The sheathing material in the tests was classified as rated sheathing which places all the OSB samples used in the tests in the category of “other graded wood structural panels” in Table D2 – 1 of AISI S213 (Figure 28). This is dependent on the quality of wood and will be shown on the stamp of the product. For the specimens that were tested in this report all but specimens No. 7 &

8 were unblocked with the load parallel to unblocked edges and continuous panel joints. For the blocked case, all screw spacing was at 152 mm (6in) o/c. It is shown that the design values proposed in the AISI S213 (2007) and AISI S400 Standard (2015) for the most part overestimate the shear strength of the diaphragm configurations, considering that the values implemented for the floor configuration correspond also to a thinner sheathing. In addition, these design values provided by Lum (LGSEA 1998) refer to plywood sheathing and there is no factor taking into account the size of the sheathing screws. These limitations do not allow for design predictions to be made corresponding to the diaphragm specimens tested; however, these are the only design values available at present in the AISI standards.

Table D2-1
United States and Mexico
 Nominal Shear Strength (R_n) for Diaphragms with Wood Sheathing^{1,4}
 (Pounds Per Foot)

Membrane Material	Screw Size	Thick-ness (In.)	Blocked				Unblocked	
			Screw spacing at diaphragm boundary edges and at all continuous panel edges (In.)				Screws spaced maximum of 6" on all supported edges	
			6	4	2.5	2	Load perpendicular to unblocked edges and continuous panel joints	All other configurations
			Screw spacing at all other panel edges (In.)					
6	6	4	3					
Structural I	See note 2	3/8	768	1022	1660	2045	685	510
		7/16	768	1127	1800	2255	755	565
		15/32	925	1232	1970	2465	825	615
C-D, C-C and other graded wood structural panels ³	See note 2	3/8	690	920	1470	1840	615	460
		7/16	760	1015	1620	2030	680	505
		15/32	832	1110	1770	2215	740	555

1. For SI: 1" = 25.4 mm, 1 foot = 0.305 m, 1 lb = 4.45 N.
2. No. 8 screws (minimum) shall be used when framing members have a designation thickness of 54 mils or less and No. 10 screws (minimum) shall be used when framing members have a designation thickness greater than 54 mils.
3. Wood structural panels shall conform to DOC PS-1 and PS-2.
4. For wood structural panel sheathed diaphragms, tabulated R_n values shall be applicable for short-term load duration (wind or seismic loads). For other in-plane lateral loads of normal or permanent load duration as defined by the AF&PA NDS, the values in the table above for wood structural panel sheathed diaphragms shall be multiplied by 0.75 (normal) or 0.67 (permanent).

Figure 28: Table D2-1 in AISI S213 (2007) or Table F2.4-1 in AISI S400 (2015)

10-Conclusions

In this technical report, an experimental program aimed at the characterization of the seismic response of CFS framed wood sheathed diaphragm systems was described in detail. Results were presented for eight diaphragm specimens representing typical floor and roof assemblies of a CFS framed building subjected to monotonic and reversed cyclic loading. Two monotonic tests were also included of the bare steel framing for the floor and roof assemblies. The main findings of the tests are summarised herein:

- ✓ Fastening around the full perimeter of the panels (blocked diaphragm) increases the diaphragm's strength considerably.
- ✓ Changing the screw size leads to different screw connection behaviour. The failure mode shifts from shearing of screws to wood bearing as the screw diameter is increased.
- ✓ As tested, the bare steel frame contribution to shear strength and stiffness is negligible.
- ✓ Limited information provided in the Standards (AISI S213 2007 & S400 2015) prohibited a meaningful comparison between calculated and experimental data. However, reasonable calculated deflection values were obtained by using the shear wall deflection equation (Eq. 1.2 in this report) and by assuming elastic diaphragm response.
- ✓ A more thorough evaluation of a method to predict diaphragm deformation is warranted accounting for more than a simply supported case.
- ✓ The range of diaphragm configurations included in the shear strength tables of the AISI standards needs to be widened to capture the effect of all construction variables, e.g. screw size of #12.
- ✓ T&G panels should be considered as a structural detail not only for the floor but also for the roof diaphragm design as they improve construction conditions and ensure a level of shear resistance of the specimen at large displacements.

From the experiments conducted for this project, it is evident that more diaphragm testing is necessary involving parameters, such as sheathing screw spacing, load direction and panel

type (i.e. plywood), for a complete database to be available to professional engineers. Further testing would also allow for a reassessment of the diaphragm deflection equation and of the amplification factor for the unblocked diaphragm cases currently in effect in the AISI S400 Standard (2015). Given the expense of testing on this scale, it is also suggested that numerical models that capture the behaviour observed during these tests be developed for the analysis of CFS framed diaphragms. These models can be calibrated with respect to the test data presented herein, and then used in subsequent parametric studies.

11-References

- ASCE/SEI 7-10 (2010). “Minimum Design Loads for Buildings and Other Structures”. American Society of Civil Engineers, Reston, VA, USA.
- AISI (2007). “AISI S213-07, North American Standard for Cold-Formed Steel Framing – Lateral Design”. American Iron and Steel Institute. Washington, DC, USA.
- AISI (2012). “AISI S100, North American Specification for the Design of Cold - Formed Steel Structural Members”. American Iron and Steel Institute. Washington, DC, USA.
- AISI (2013). “AISI S907-13, Test Standard for Cantilever Test Method for Cold-formed Steel Diaphragms”. American Iron and Steel Institute. Washington, DC, USA.
- AISI (2015). “AISI S400, North American Standard for Seismic Design of Cold-Formed Steel Structural Systems”. American Iron and Steel Institute. Washington, USA; 2015.
- AISI (2015). “AISI S240, North American Standard for Cold-Formed Steel Structural Framing”. American Iron and Steel Institute. Washington, USA; 2015.
- APA (2007). “Diaphragms and Shear Walls”. The Engineered Wood Association. Design/Construction Guide Form No. L350A.
- ASTM (2007a). “A370 - 7a Standard Test Methods and Definitions for Mechanical Testing of Steel Products”. American Society for Testing and Materials, West Conshohocken, PA.
- ASTM (2007). “D4442 - 07 Standard Test Methods for Direct Moisture Content Measurement of Wood and Wood Base Materials”. American Society for Testing and Materials, West Conshohocken, PA.
- Blais, C. (2006). “Testing and Analysis of Light Gauge Steel Frame / 9mm OSB Wood Panel Shear Walls”. M.Eng. Thesis, Department of Civil Engineering & Applied Mechanics, McGill University, Montreal, QC, Canada.
- Blais, C. (2006). “Testing and Analysis of Light Gauge Steel Frame / 9mm OSB Wood Panel Shear Walls”. M.Eng. Thesis, Department of Civil Engineering & Applied Mechanics, McGill University, Montreal, QC, Canada.
- Boudreault, F.A. (2005). “Seismic Analysis of Steel Frame / Wood Panel Shear Walls”. M.Eng. Thesis, Department of Civil Engineering and Applied Mechanics, McGill University, Montreal, Qc, Canada.
- Branston, A.E. (2004). “Development of a Design Methodology for Steel Frame / Wood Panel Shear Walls”. M.Eng. Thesis, Department of Civil Engineering and Applied Mechanics, McGill University, Montreal, Qc, Canada.
- Chen, C.Y. (2004). “Testing and Performance of Steel Frame / Wood Panel Shear Walls”. M.Eng. Thesis, Department of Civil Engineering and Applied Mechanics, McGill University, Montreal, Qc, Canada.

- Brignola, A., Pampanin, S. and Podestà, S. (2012). “Experimental Evaluation of the In-Plane Stiffness of Timber Diaphragms”. *Earthquake Spectra* 28.4 (2012): 1687-1709.
- CSA O86-09 (2009). “Engineering design in wood”. Canadian Standards Association. Ontario, Canada.
- CSA S16-14 (2014). “Design of steel structures”. Canadian Standards Association. Ontario, Canada.
- CSA S136-07 (2007). “North American Specification for the Design of Cold-Formed Steel Structural Members”. Canadian Standards Association, Mississauga, ON, Canada.
- CSI, SAP2000 V.14 (2009). “Linear and Non-linear Static and Dynamic Analysis and Design of Three-Dimensional Structures Basic Analysis Reference Manual”. Computers and Structures, Inc., Berkeley, California, USA.
- Dolan, J. D., and Madsen B. (1992). “Monotonic and Cyclic Tests of Timber Shear Walls”. *Canadian Journal of Civil Engineering* 19.3 : 415-422.
- Krawinkler, H., Parisi, F., Ibarra, L., Ayoub, A., Medina, R. (2000). “Development of a Testing Protocol for Woodframe Structures”. Report W-02 covering Task 1.3.2, CUREE/Caltech Woodframe Project. Consortium of Universities for Research in Earthquake Engineering (CUREE). Richmond, CA, USA.
- Leng, J., Schafer, B.W. and Buonopane, S. G. (2013), “Modeling the Seismic Response of Cold-formed Steel Framed Buildings: Model Development for the CFS-NEES Building”, *Proceedings of the Annual Stability Conference Structural Stability Research Council*, St. Louis, Missouri.
- LGSEA (1998). “Lateral Load Resisting Elements: Diaphragm Design Values”. Tech Note 558b-1, LightGauge Steel Engineers Association, Washington, DC, 1998.
- Liu, P., Peterman, K.D., Yu, C., Schafer, B.W. (2012). “Cold-Formed Steel Shear Walls in Ledger-Framed Buildings”. *Annual Stability Conference, Structural Stability Research Council*, April 2012, Grapevine, Texas, USA.
- McKenna, F. (1997). “Object-oriented finite element programming: Frameworks for analysis, algorithms, and parallel computing”. Ph.D. thesis, University of California, Berkeley, California.
- Madsen, R.L., Nakata, N., Schafer, B.W. (2011). “CFS-NEES Building Structural Design Narrative”. CFS-NEESRR01.
- NAHB Research center (1999). “Innovative Residential Floor Construction: Horizontal Diaphragm Values for Cold-formed Steel Framing”. U.S. Department of Housing and Urban Development.
- National Research Council of Canada (NRCC) (2010). “National Building Code of Canada 2010, 13th Edition”. Ottawa, ON, Canada.

- National Research Council of Canada (NRCC) (2005). “National Building Code of Canada 2005, Ottawa, ON, Canada.
- NDS (1991). “National Design Specification for Wood Construction”. ANSI/NFoPA, American Forest & Paper Association, 1991.
- Peterman, K.D. (2014). “Behaviour of Full-Scale Cold-Formed Steel Buildings Under Seismic Excitations”. PhD Thesis, Johns Hopkins University, Baltimore, Maryland.
- Rokas, D. (2005). “Testing of Steel Frame / 9.5 mm CSP Wood Panel Shear Walls”. Project Report, Department of Civil Engineering and Applied Mechanics, McGill University, Montreal, Qc, Canada.
- Schafer, B.W., Ayhan, D., Leng, J., Liu, P., Padilla-Llano, D., Peterman, K.D., Stehman, M., Buonopane, S.G., Eatherton, M., Madsen, R., Manley, B., Moen, C.D., Nakata, N., Rogers, C. and Yu, C. (2014). “The CFS-NEES Effort: Advancing Cold-formed Steel Earthquake Engineering”. Tenth U.S. National Conference on Earthquake Engineering, July 21-25, 2014, Anchorage, Alaska.
- Serrette, R.L., and Chau, K. (2003). “Estimating the Response of Cold-Formed Steel-Frame Shear Walls”. Santa Clara University, Santa Clara, CA.
- Tissell, J. R. and Elliot, J. R. (2004). “Plywood Diaphragms”. Research Report 138, American Plywood Association (APA), Tacoma, Washington.
- TECO (2008). “TECHTIP. Design Capacities for Oriented Strand Board”. Retrieved Oct 30th, 2015, from http://www.tecotested.com/techtips/pdf/tt_osbdesigncapacities.



American Iron and Steel Institute

25 Massachusetts Avenue, NW
Suite 800
Washington, DC 20001

www.steel.org

